



Munich Personal RePEc Archive

A Study of Financial Cycles and the Macroeconomy in Taiwan

Chen, Nan-Kuang and Cheng, Han-Liang

Central Bank of the ROC (Taiwan), National Taiwan University

23 June 2020

Online at <https://mpra.ub.uni-muenchen.de/101296/>
MPRA Paper No. 101296, posted 10 Jul 2020 15:37 UTC

A Study of Financial Cycles and the Macroeconomy in Taiwan*

Nan-Kuang Chen[†] and Han-Liang Cheng[‡]

This version: June, 2020

Abstract

This paper studies the characteristics of financial cycles (credit and house prices) and their interactions with business cycles in Taiwan. We employ multivariate structural time series model (STSM) to estimate trend and cyclical components in real bank credit, real house prices, and real GDP. We find that financial cycles are roughly twice the length of the business cycles, and house price cycles lead both credit and business cycles. Nevertheless, the estimated length of business and financial cycles in Taiwan is much shorter than those in industrialized economies. We then use machine learning to evaluate the importance of a macroeconomic variable that predicts downturns of financial cycles, by conducting both in-sample fitting and out-of-sample forecasting. Those macro variables selected by machine learning reflects Taiwan's close linkage in trades and financial interdependence with other countries such as China and spillover effects from the Fed's monetary policy.

Key words: financial cycle, credit, house prices, wavelet analysis, machine learning

*The views expressed herein are those of the authors and do not necessarily reflect the official opinions of Central Bank of the ROC (Taiwan).

[†]Central Bank of the ROC (Taiwan) and Department of Economics, National Taiwan University; e-mail: nankuang@ntu.edu.tw.

[‡]Central Bank of the ROC (Taiwan); e-mail: d94323006@ntu.edu.tw.

In the environment that has prevailed for at least three decades now, it is simply not possible to understand business fluctuations and their policy challenges without understanding the financial cycle (Borio; 2014).

1 Introduction

In the aftermath of the global financial crisis (GFC), the boom-bust cycles of financial variables have gained considerable attention. The important role of financial variables in driving economic activity has spurred a rich line of research examining the interconnectedness of credit cycles and boom-busts of asset prices, and its macroeconomic consequences. Recent evidence shows that sustained rapid credit growth combined with large increases in asset prices before the GFC was followed by deep and severe recessions amplified through credit crunch and asset price bust (Mishkin (2008), Mian and Sufi (2009), Bordo and Haubrich (2010)). Moreover, the long-term historical evidence also suggested that financial crises have been preceded by credit and housing price booms (Reinhart and Rogoff (2009), Schularick and Taylor (2012), Jorda et al. (2013)).

The transmission mechanism between credit and asset prices have been well-documented.¹ As a result, the boom-busts of these two aggregate variables are coined as “financial cycles.” Recently, several works have identified several key stylized facts about the financial cycles mainly for industrialized economies (Drehmann et al., 2012; Claessens et al., 2012; Borio, 2014). First, the financial cycles can be well characterized by credit and property prices, which behave distinctively from the business cycles.² Second, the length and amplitude of the financial cycles greatly exceed those of the business cycles, i.e., the financial cycle has a much lower frequency than the business cycle.³ Third, peaks in the financial

¹See, for example, Dell’Ariccia et al. (2008), Duca et al. (2010, 2011), Kiyotaki and Moore (1997), Chen (2001), Iacoviello (2005).

²As for the stock price, it has much a higher degree of synchronization with the business cycle than credit and house price cycles do.

³Given the stylized facts of financial cycles for industrialized economies outlined above, however, there is a heterogeneity among these countries. For example, in some cases the financial cycles of Germany are found to be substantially shorter than other European countries. However, the reason for this finding is yet to be clear.

cycle tend to coincide with episodes of systemic financial distress, and recessions associated with house price busts tend to be longer and much deeper than other recessions. Therefore, a better understanding of the financial cycles is essential for policymakers to address the issues related to financial stability.

In this paper, we try to characterize the regularities of financial cycles and their relationship with business cycles in Taiwan. Taiwan is a small-open economy, with trade openness, the ratio of total trades to GDP, maintaining well above 100% since 2004. Thus, the macroeconomic dynamics in Taiwan are greatly influenced by exogenous shocks from other parts of the world. Among its largest trading partners, China (including Hong Kong), US, and Europe respectively account for 29.8%, 13.8%, and 11% of Taiwan's total trades in June 2019. As argued by Rey (2013) and Miranda-Agrippino and Rey (2019), the monetary policy shocks of the Fed and other main central banks may significantly induce comovements in the international financial variables that characterize the "Global Financial Cycle." As a result, financial cycles in Taiwan can also be substantially affected by the economic activity and monetary policy of these large economies.

The main econometric method used in this paper is the multivariate structural time series model (STSM), which is a version of unobservable components model (UCM) introduced by Harvey and Koopman (1997) and Runstler (2004). The model takes into account of the interactions of these time series and allows for jointly decomposing the time series into trends and cyclical components at different frequencies and also account for possible common trends and cycles. We also use the Wavelet analysis to measures coherence in the time-frequency domain and the time-varying lead/lag relation between pairwise time series.

We then try to investigate the macroeconomic factors that explain the dynamics of financial cycles estimated from the multivariate STSM. After identifying the upturns and downturns of financial cycles, we then evaluate the importance of a macroeconomic variable in predicting the downturns of financial cycles, for both in-sample fitting and out-of-sample forecasting. The method we employ is machine learning, including random forest and boosting, which can include as much as information while maintaining the power and precision of the estimation.

The main findings are as follows. First, credit and house price share "similar" cycles,

i.e., the frequency and persistence of the two cycles are significantly similar. This is also evidenced by the estimates of high coherence between the two cycles. Nevertheless, the peaks, troughs, and scales of the trends and cycles for credit and house prices can still differ from each other. Second, financial cycles are roughly twice the length of the business cycles, i.e., financial cycles in Taiwan do have a lower frequency than the business cycles. Nevertheless, the estimated length of financial cycles in Taiwan is substantially shorter than those in industrialized economies identified by Drehmann et al. (2012), Schuler et al. (2015), and Runstler and Vlekke (2018), which echoes the findings of four east Asian economies in Pontines (2017).⁴

Third, the average coherences among the three time series show that credit and house price cycles are more closely correlated than other pairs. Also, the estimated average phase shifts indicate that GDP leads credit cycles and lags house price cycles, i.e., house price cycles lead both credit and GDP cycles. This may suggest that the boom-bust cycles of house price in Taiwan appears not entirely credit and economic fundamentals generated, but also substantially affected by other factors. We check these results using the Wavelet analysis, and find that the mean properties of the Wavelet analysis regarding pairwise correlations and lead/lag relations at different time-frequency domains are consistent with those of our multivariate STSM.

Finally, we apply machine learning to in-sample fitting and out-of-sample forecasting for macroeconomic variables that predict the downturns of financial cycles in Taiwan. For in-sample fitting, the best macroeconomic variables that explain the downturns of financial cycles include not only domestic economic fundamentals and monetary policy, but also economic outlooks of China as well as US monetary policy and term spread. As for out-of-sample forecasting, we find that all top 12 important variables for in-sample fitting that explain the downturns of house prices and credit are almost all included in results of out-of-sample forecasting with forecasting horizon $h = 1$ to 4. Summarizing results from in-sample fitting as well as out-of-sample forecasting, we find that, as a small-open economy, Taiwan's financial cycles are deeply affected by fluctuations in international financial and economic conditions, particularly reflecting Taiwan's close ties in trades and

⁴Note that due to data limitation, Pontines (2017) examines GDP and equity prices for Hong Kong, Malaysia, Philippines and Thailand. House prices were available only for Hong Kong.

financial interdependence with the world economy, and spillover effect of the US monetary policy.

The rest of the paper is organized as follows. Section 2 discusses the related literature. Section 3 describes the data sources. Section 4 outlines the econometric model. Section 5 presents the estimation results of the univariate and multivariate STSM. Section 6 identifies the upturns and downturns of financial cycles. Section 7 uses machine learning to predicting the downturns of financial cycles, for both in-sample fitting and out-of-sample forecasting. Section 8 concludes.

2 Related Literature

Existing works have used various methods to characterize the financial cycles. Most of these studies tend to use univariate techniques, which include turning points analysis (e.g. Claessens et al. (2011, 2012), Drehmann et al. (2012)), frequency-based filter methods (e.g. Drehmann et al. (2012), Aikman et al. (2015)), and spectral analysis (e.g. Pontines (2017), Schuler et al. (2015)). These empirical studies have found strong linkages between financial cycles and business cycles.

On the other hand, the multivariate STSM approach (Harvey and Koopman (1997) and Runstler (2004)) we adopt here has so far only been employed by a few studies, including Chen et al. (2012) and Runstler and Vlekke (2018). The multivariate model-based STSM has several advantages over alternative approaches.

First, use of the HP and band-pass filters (Drehmann et al. (2012), Aikman et al. (2015)) requires pre-specified frequency bands, which may risk losing parts of cyclical dynamics or obtaining spurious cycles (Murray (2003)). In comparison to these non-parametric filter approaches, this model-based method does not rely on prior assumptions on the length of each cycle, which can avoid potential distortions caused by misspecification, and is much more flexible for studying the financial cycles. Second, Some authors have used univariate UCM. However, univariate models do not appropriately account for the endogenous interactions of trends and cycles in asset prices, credit and output. The multivariate STSM can simultaneously decompose all the time series into

trend and cyclical components, and accounts for the possible common trends and cycles. Finally, using this estimated model parameters can provide a more coherent and systematic measure of cyclical correlations, which can reveal leading and lagging relationships among credit, house prices, and GDP.

As for the method to explain the upturns or downturns of financial cycles, we consider two types of machine learning algorithms – random forest (Breiman (2001)) and boosting (Schapire (1999)). These two algorithms are two of the most popular techniques of learning models that can improve prediction performances. By construction, a random forest consists of a large ensemble of de-correlated decision trees. Depending on the nature of problem at hand, either high-dimensional classification or regression problems, each decision tree is capable of producing a response when presented with a set of predictor values. Corresponding to our problem in this paper, the response involves the classification of a set of independent predictor values, i.e., classifying as a downturn or an upturn. Then, the ensemble of decision trees vote for the most popular class by averaging their predictions. On the other hand, boosting is based on a different strategy of ensemble formation. Basically, it is an iterative process by adding new models to the ensemble sequentially. At each particular iteration, a new base-learner model is trained with respect to the error of the whole ensemble learnt so far. In sum, boosting combines models that do not perform particularly well individually into one with much improved properties.

These algorithms are able to deal with a large number of predictors, perform estimation and variable selection simultaneously, and may improve prediction accuracy. They are now increasingly applied to the predictions of turning points of business cycles (see, for example, Raffinot (2017) and Berge (2015)).

3 Data Sources

The main observations for studying financial cycles in Taiwan include quarterly real GDP (Y_t), real domestic total bank credit to private sector (C_t), and an index of real residential property prices (Q_t), ranging from 1994Q2 to 2017Q3. The real total bank credit and real residential property prices are deflated by the CPI. GDP and CPI come from the Directorate General of Budget, Accounting and Statistics (DGBAS). The residential

property prices are obtained from Xinyi house price index, which is the most widely used house price index and has the longest time series available in Taiwan. Finally, total bank credit is obtained from the Central Bank of the Republic of China (Taiwan).

As for studying the macroeconomic factors that explain the dynamics of financial cycles in Taiwan, a total of 74 macroeconomic variables are used, with sample periods ranging from 1995Q2 to 2017Q3⁵. Besides domestic macroeconomic and monetary variables, we also include indicators reflecting international macroeconomic outlooks, monetary policy of the Fed, and net capital inflows to Taiwan. The variables are seasonally adjusted if the officially released data were not. We then use HP filter to remove the long-term trend of each variable and use the first difference of variables as predictors.⁶

4 The Multivariate STSM

We start with describing the methodology of multivariate STSM. Consider a vector of n observable variables $\mathbf{y}_t = (y_{1,t}, y_{2,t}, \dots, y_{n,t})'$, where $n = 3$ in our case, which are GDP, credit, and house prices. The vector of time series \mathbf{y}_t can be decomposed into three unobservable components: trends $\boldsymbol{\mu}_t$, cyclical components \mathbf{y}_t^c , and irregular components $\boldsymbol{\varepsilon}_t$,

$$\mathbf{y}_t = \boldsymbol{\mu}_t + \mathbf{y}_t^c + \boldsymbol{\varepsilon}_t, \quad (1)$$

where the $n \times 1$ vector $\boldsymbol{\varepsilon}_t$ of irregular components, capturing measurement noise in the observations, is normally and independently distributed with mean zero and $n \times n$ covariance matrix Σ_ε , $\boldsymbol{\varepsilon}_t \sim NID(\mathbf{0}, \Sigma_\varepsilon)$.

The $n \times 1$ vector $\boldsymbol{\mu}_t$ of stochastic trend components filters out low-frequency or long-term dynamics from the data and is assumed to follow a multivariate random walk process with a time-varying slope $\boldsymbol{\beta}_t$:

$$\boldsymbol{\mu}_t = \boldsymbol{\mu}_{t-1} + \boldsymbol{\beta}_t + \boldsymbol{\eta}_t, \quad (2)$$

$$\boldsymbol{\beta}_t = \boldsymbol{\beta}_{t-1} + \mathbf{v}_t, \quad (3)$$

⁵Note that due to limit of sample periods for a large number of variables, the estimation starts at 1995Q2.

⁶The list of all 74 variables is omitted here, but is available upon request.

where the innovations of trend and slope, $\boldsymbol{\eta}_t$ and \boldsymbol{v}_t , are also normally and independently distributed with mean zero and covariance matrices, Σ_η and Σ_v , respectively: $\boldsymbol{\eta}_t \sim NID(\mathbf{0}, \Sigma_\eta)$ and $\boldsymbol{v}_t \sim NID(\mathbf{0}, \Sigma_v)$.

The cyclical components $\mathbf{y}_t^c = (y_{1,t}^c, y_{2,t}^c, \dots, y_{n,t}^c)'$ are modelled as linear combinations of n independent stochastic cycles $\Phi_{i,t} = (\psi_{i,t}, \psi_{i,t}^*)'$, $i = 1, 2, \dots, n$. The stochastic cycles $\Phi_{i,t}$ is specified to be the bivariate stationary first-order autoregressive process:

$$\left(I_2 - \rho_i \begin{bmatrix} \cos(\lambda_i) & \sin(\lambda_i) \\ -\sin(\lambda_i) & \cos(\lambda_i) \end{bmatrix} L \right) \begin{pmatrix} \psi_{i,t} \\ \psi_{i,t}^* \end{pmatrix} = \begin{pmatrix} \vartheta_{i,t} \\ \vartheta_{i,t}^* \end{pmatrix}, \quad (4)$$

where the cyclical innovations $(\vartheta_{i,t}, \vartheta_{i,t}^*)'$ are serially and mutually uncorrelated and assumed to follow normalized normal distribution: $(\vartheta_{i,t}, \vartheta_{i,t}^*)' \sim NID(\mathbf{0}, I_2)$. Note that the parameter $0 < \lambda_i < \pi$ represents the cycle frequency, measuring the peak of the hump-shaped auto-spectral densities, and the persistence (or decay) parameter $0 < \rho_i < 1$ represents the damping factor, determining the dispersion around the peak. The duration or length of the cycle for time series i is equal to $2\pi/4\lambda_i$. Note that specifying in this way allows for modeling cyclical comovements among the n time series in terms of phase-adjusted covariances and phase shifts between short-cycles and long-cycles.

After describing the stochastic cycles $\Phi_{i,t}$ for each time series i , we are now ready to specify the cyclical components \mathbf{y}_t^c . As outlined above, the elements of cyclical components \mathbf{y}_t^c are assumed to be driven by n independent latent stochastic cycles, and can be written as linear combinations of $\psi_{i,t}$ and $\psi_{i,t}^*$. Let $\boldsymbol{\Psi}_t = (\psi_{1,t}, \dots, \psi_{n,t})'$ and $\boldsymbol{\Psi}_t^* = (\psi_{1,t}^*, \dots, \psi_{n,t}^*)'$. The cyclical innovations $\boldsymbol{\vartheta}_t = (\vartheta_{1,t}, \dots, \vartheta_{n,t})'$ and $\boldsymbol{\vartheta}_t^* = (\vartheta_{1,t}^*, \dots, \vartheta_{n,t}^*)'$ are assumed to be uncorrelated and follow $E(\boldsymbol{\vartheta}_t \boldsymbol{\vartheta}_t') = E(\boldsymbol{\vartheta}_t^* \boldsymbol{\vartheta}_t^{*'}) = I_n$ and $E(\boldsymbol{\vartheta}_t \boldsymbol{\vartheta}_t^{*'}) = 0$. Thus, the cyclical components \mathbf{y}_t^c are given by

$$\mathbf{y}_t^c = B\boldsymbol{\Psi}_t + B^*\boldsymbol{\Psi}_t^*, \quad (5)$$

where $B = (b_{ij})$ and $B^* = (b_{ij}^*)$ are $n \times n$ matrices.

Given the above specification, the auto-covariance generating function (ACF) $\Omega_{ii}(s) = E[\Phi_{i,t} \Phi_{i,t-s}']$, $s = 0, 1, 2, \dots$ and $i = 1, 2, \dots, n$, of the stochastic cycle is given by

$$\Omega_{ii}(s) = h(s; \rho_i) \Gamma(s\lambda_i), \quad (6)$$

where

$$\Gamma(s\lambda_i) = \begin{pmatrix} \cos(s\lambda_i) & \sin(s\lambda_i) \\ -\sin(s\lambda_i) & \cos(s\lambda_i) \end{pmatrix}, \quad (7)$$

and the scalar function is $h(s; \rho_i) = \rho_i^s / (1 - \rho_i^2)$.

Most existing works using UCM or STSM tend to impose the assumption of “similar cycles” (Koopman and Lucas (2005), Chen et al. (2012)), i.e., the frequency and persistence of all the cycles are the same, $\lambda_i = \lambda$ and $\rho_i = \rho$ for $i = 1, \dots, n$. Given the similar cycles restriction, the peaks, troughs, and scales of the trends and cycles, as determined by the variance and covariance matrices of the disturbances driving the components, can still be different from each other. An advantage of making this assumption is that the ACF in (6) can be expressed as a simple closed form

$$\Omega_{ii}(s) = h(s; \rho) r_{ij} \cos(\lambda(s - \theta_{ij})), \quad (8)$$

where $r_{ij} = \sqrt{b_{ij}^2 + b_{ij}^{*2}}$ and $\theta_{ij} = \lambda^{-1} \arctan(b_{ij}^*/b_{ij})$.

In this paper we allow for non-similar cycles, i.e., λ_i and ρ_i can be different for $i = 1, \dots, n$. We will test for the hypothesis of similar cycles pairwise and then decide whether to impose this restriction. Allowing for non-similar cycles will pose difficulties in computing the ACF of \mathbf{y}_t^c , because the closed form expression of $\Omega_{ii}(s)$ in (8) is no longer available. To characterize cyclical comovement, we follow Runstler and Vlekke (2018) by computing the multivariate spectral generating function $G^c(\omega)$ of \mathbf{y}_t^c to derive the average frequencies of cyclical components $y_{i,t}^c$ and also the average coherences and phase shifts among these time series from the integrals

$$\left(\int_0^\pi \sqrt{G_{ii}^c(\omega) G_{jj}^c(\omega)} \right)^{-1} \int_0^\pi \varphi_{ij}(\omega) \sqrt{G_{ii}^c(\omega) G_{jj}^c(\omega)} d\omega, \quad (9)$$

where $G_{ij}^c(\omega)$ is an element of $G^c(\omega)$. The average frequencies for the case of non-similar cycles is denoted as λ_i^G , thus the (annual) average cycle length of time series i is given by $2\pi/4\lambda_i^G$.⁷

The econometric model consists of (1), (2), (3), and (5), with elements $\Phi_{i,t} = (\psi_{i,t}, \psi_{i,t}^*)'$ of vectors $\Psi_t = (\psi_{1,t}, \dots, \psi_{n,t})'$ and $\Psi_t^* = (\psi_{1,t}^*, \dots, \psi_{n,t}^*)'$, each following the stochastic

⁷The details for computing the average frequencies λ_i^G and the average coherences and phase shifts can be referred to the appendix of Runstler and Vlekke (2018).

processes defined by (4). The parameters are given by matrices Σ_ε , Σ_η , Σ_ν , B , and B^* , together with ρ_i and λ_i , $i = 1, \dots, n$. All the innovations ε_t , η_t , ν_t , ϑ_t , and ϑ_t^* are assumed to be mutually uncorrelated.

To estimate the model, we rewrite the above equations in state-space form

$$\mathbf{y}_t = \mathbf{P}\boldsymbol{\omega}_t + \boldsymbol{\varepsilon}_t, \quad (10)$$

$$\boldsymbol{\omega}_t = \mathbf{Q}\boldsymbol{\omega}_{t-1} + \boldsymbol{\tau}_t, \quad (11)$$

where equation (10) connects the observed variables \mathbf{y}_t to the unobserved state vector $\boldsymbol{\omega}_t$, while equation (11) characterizes the law of motion for the unobserved state vector. The state vector $\boldsymbol{\omega}_t$ includes the unobserved components $\boldsymbol{\mu}_t$, $\boldsymbol{\beta}_t$, Ψ_t , and Ψ_t^* . The system matrices \mathbf{P} and \mathbf{Q} that determine the dynamic properties of \mathbf{y}_t , together with the variance matrices $\boldsymbol{\varepsilon}_t$ and $\boldsymbol{\tau}_t$, contain the parameters of the model. We describe in more details the state-space matrix form in Appendix A.

We estimate the model parameters by using maximum likelihood and apply the prediction error decomposition of the Kalman filter. For comparison, we also estimate the univariate STSM. Note that the univariate STSM is jointly estimated for all time series in (1). Compared to multivariate STSM, the interactions among the three time series in univariate STSM are not considered. Thus, the cyclical component under univariate STSM can be simplified as $y_{i,t}^c = b_i\psi_{i,t}$ in (5) with a scalar b_i , while $\psi_{i,t}^*$ serves as an auxiliary variable.

5 Estimation Results

5.1 Similar Cycles Restriction Test

The first step of our empirical estimation is to test for pairwise similar dynamics among GDP, credit, and house prices. Recall that λ_i represents the frequency of the cycle and ρ_i measures the persistence of the cycle. The null hypothesis of the similar cycles is to impose $\lambda_i = \lambda_j$ and $\rho_i = \rho_j$ on restricted univariate or multivariate STSM. The statistic of the likelihood ratio (LR) test is given by $LR = 2(L_U - L_R)$, where L_U is log-likelihood of the unrestricted model and L_R is log-likelihood of the restricted model.

We estimate both the univariate and multivariate STSM to obtain the model parameters. We present the LR test results of the null $\lambda_2 = \lambda_3$ and $\rho_2 = \rho_3$ in Table 1.⁸ The LR test suggests that, either under univariate or multivariate model, the similar cycle hypotheses of credit and house price cannot be rejected at the 1% significance level. The LR tests for other pairs of similar cycle hypotheses are rejected (not reported here).

We therefore impose the restriction that credit and house price cycles share similar cycles on subsequent estimates, and allow for business cycles to be different from financial cycles.

Table 1a Similar Cycle Restriction Test of Credit and House Prices: Univariate STSM

	Stochastic Cycle		Trend Innovations		
	ρ	$2\pi/4\lambda$		σ_η	σ_v
$\psi_{1,t}$	0.3877	3.981	Y_t	0.0004	0.0013
$\psi_{2,t}$	0.2517	8.886	C_t	0.001	0.0036
$\psi_{3,t}$	0.2517	8.886	Q_t	0.001	0.0056
LR test	$2 \times (1277.5 - 1277.4) = 0.2 < 9.2$				

Note: Imposing $\lambda_2 = \lambda_3$ and $\rho_2 = \rho_3$. The critical value of $\chi^2(2)$ at 1% significance level is 9.2.

Table 1b Similar Cycle Restriction Test of Credit and House Prices: Multivariate STSM

	Stochastic Cycle		Trend Innovations		
	ρ	$2\pi/4\lambda$		σ_η	σ_v
$\psi_{1,t}$	0.3456	2.484	Y_t	0.0003	0.0001
$\psi_{2,t}$	0.2563	8.814	C_t	0.001	0.001
$\psi_{3,t}$	0.2563	8.814	Q_t	0.0006	0.0002
LR test	$2 \times (1298.2 - 1291.2) = 14.00 < 15.1$				

⁸To avoid an overly smooth slope and make sure that the maximum likelihood estimation is able to converge and attain a maximum value, we restrict the values of standard deviations of innovations ε_t , σ_η , and σ_v for both the univariate and multivariate STSM (Rustler and Vlekke (2018)).

Note: If credit and house prices share similar dynamics, the identifiability is achieved from $B_{13} = B_{23}^* = 0$. See Runstler and Vlekke (2018) for more details. We impose $\lambda_2 = \lambda_3$, $\rho_2 = \rho_3$, $B_{13} = 0$, $B_{23}^* = 0$, and $\sigma_\eta = 0.0006$. The critical value of $\chi^2(5)$ at 1% significance level is 15.1.

5.2 Estimation Results of Univariate and Multivariate STSM

Table 2 shows the estimation results of average length of cycles for the univariate and multivariate STSM.⁹ For univariate STSM, similar cycles restriction results in the same average frequencies, $\lambda_2^G = \lambda_3^G$. The second column of Table 2 shows that the average length of credit and house price cycle given by $2\pi/4\lambda^G$ is 6.75 years, while that of GDP is 3.46 years.

Table 2 Average Length of Cycles

	Univariate STSM	Multivariate STSM
	$2\pi/4\lambda^G$	$2\pi/4\lambda^G$
Y_t	3.46	3.46
C_t	6.75	6.63
Q_t	6.75	5.80

As for multivariate STSM, the cyclical component \mathbf{y}_t^c turns out to be a mixture of $(\psi_{i,t}, \psi_{i,t}^*)$, $i = 1, 2, \dots, 3$, with loadings given by B and B^* . Thus, even if we impose the restriction of similar cycles between credit and house prices, i.e., $\lambda_2 = \lambda_3$ and $\rho_2 = \rho_3$, the computed average frequencies λ_i^G , $i = 1, 2, \dots, 3$, from (9) can still be different. Therefore, the lengths of cycles for credit and house prices may differ from each other. As presented in the third column of Table 2, the average lengths of credit and house prices are respectively 6.63 and 5.80 years, which are longer than that of GDP (3.46 years).

⁹For the purpose of comparison, we also estimate Hodrick-Prescott (HP) filter, frequency-based filter, ARMA spectral analysis, univariate UCM, and univariate STSM to measure financial and business cycles. There are some differences between these methods and the multivariate STSM. As mentioned in Introduction, these alternative methods have obvious shortcomings compared to multivariate STSM. The results are available upon request.

In summary, no matter which model is used, financial cycles are roughly twice the length of business cycles. Therefore, the financial cycles in Taiwan do have a lower frequency than the business cycle. Nevertheless, the estimated lengths of business cycles as well as financial cycles in Taiwan are clearly much shorter than those in industrialized economies identified by Aikman et al. (2015), Drehmann et al. (2012), Schuler et al. (2015), and Runstler and Vlekke (2018), which resembles the findings of four east Asian economies in Pontines (2017).¹⁰

We depict the estimated financial and business cycles under multivariate STSM in Figure 1a. A clear pattern of the figure is that house prices lead credit and house prices and credit are more closely correlated, compared to their respective correlation with GDP.

Moreover, by taking an average of credit and house price cycles based on multivariate STSM, Figure 1b shows the financial cycles in Taiwan. Note that the peak of financial cycle coincides with the beginning of the GFC.

[Figure 1 here]

To gain more insights about the financial cycles, we compute the lead-lags and correlations based on the multivariate STSM, presented in Table 3. Firstly, in the upper triangular part of Table 3, we present the phase shifts (in annual terms) of the model. Reading from the first row, the average phase shifts indicate that GDP leads credit cycles by 0.80 years, and lags house price cycles by 1.39 years, implying that house price cycles lead both credit and GDP cycles. This suggests that the boom-bust cycles of house price

¹⁰Why are business cycles in Taiwan substantially shorter than those in other industrialized economies? Rand and Tarp (2002) study the nature and characteristics of short-run macroeconomic fluctuations for 15 developing countries, and find that their business cycles are generally shorter than their developed counterparts. They argue that this is because shocks originating in developed countries are important drivers of short-run output fluctuations in developing countries. Taiwan is a highly small open economy, and thus its economic activity is deeply affected by external shocks from other economies. Monetary policy and business fluctuations from advanced economies and trading partners are the main sources of these external shocks, which makes Taiwan's business cycles exposed to external shocks and fluctuate more frequently than industrialized economies.

in Taiwan appears not entirely credit and economic fundamentals generated, but may also be substantially affected by other factors.

Table 3 Estimation Results of Average Coherences and Phase Shifts

Coherence	Phase Shifts		
	Y_t	C_t	Q_t
Y_t	--	0.80	-1.39
C_t	0.45	--	-0.59
Q_t	0.44	0.56	--

Note: The lower triangular matrix shows the average coherences, while the upper triangular part shows the average phase shifts (in annual terms) from the estimates of multivariate STSM.

Next, the lower triangular part of the matrix in Table 3 shows the average coherences among the three time series from the estimates of multivariate STSM. It appears that credit and house price cycles are more closely correlated, with a coherence of 0.56, while estimates of coherence of GDP with financial cycle range from 0.44 to 0.45. This results are consistent with our similar cycles restriction that credit and house prices share similar cyclical dynamics.

In the previous subsection, the similar cycle restriction test finds that credit and house price cycles share similar cycles, while business cycles appear to behave differently from financial cycles. The results from Table 3 are consistent with our findings in the previous subsection where the estimated coherence shows that credit and house price cycles are more closely correlated, while estimates of coherence of GDP with financial cycle are lower.

To conduct residual diagnostics of the Multivariate STSM, we employ the BDS test and the distribution test to check whether the prediction errors are independent and identically distributed (i.i.d.) and normally distributed.¹¹ According to Brock et al. (1996), the BDS test checks whether the prediction errors are i.i.d.. As Table 4a shows, all BDS Statistics of prediction errors cannot reject the null hypothesis at 1% significance level at different

¹¹We use the package of `eviews` to conduct both the BDS test and the distribution test.

dimensions, implying that the prediction errors of the estimated Multivariate STSM are i.i.d..

Table 4a BDS Statistics- Multivariate STSM

Dimension	GDP		Credit		House price	
	BDS Stat.	P-value	BDS Stat.	P-value	BDS Stat.	P-value
2	0.022	0.05	-0.001	0.93	0.019	0.05
3	0.026	0.12	-0.002	0.98	0.031	0.05
4	0.029	0.14	-0.005	0.93	0.033	0.07

Note: P-values are obtained by using bootstrap.

We then use Lilliefors (1967) and Cramer-von Mises (see e.g. Thode, 2002) methods to test whether prediction errors are normally distributed. Table 4b shows that all statistics cannot reject the null hypothesis at 1% significance level, implying that the prediction errors of the estimated Multivariate STSM are normally distributed.

Table 4b Distribution Tests- Multivariate STSM

Method	GDP			Credit		
	Stat.	Adj. stat.	P-value	Stat.	Adj. stat.	P-value
Lilliefors	0.08	-	> 0.1	0.06	-	> 0.1
Cramer-von Mises	0.12	0.13	0.05	0.06	0.06	0.36
House price						
Method	Stat.	Adj. stat.	P-value			
Lilliefors	0.07	-	> 0.1			
Cramer-von Mises	0.06	0.06	0.35			

Note: P-values are reported for the adjusted statistics.

5.3 The Wavelet Analysis

We also examine whether the relationship between financial cycles and business cycles are changing over time, by adopting a time-varying approach for pairwise comovement of the growth rate of house price, credit, and GDP in the time-frequency space. Traditional state-space model of cyclical analysis cannot capture such historical information because they do not consider the time-varying characteristics of the cycles.

Following Hanus and Vacha (2020), we use the wavelet coherence to evaluate the pairwise comovement of credit, house price and GDP, and the phase difference to analyze the time-varying lead/lag relation of these variables in specific frequencies. The wavelet analysis avoids imposing ex-ante restrictions on the frequency range on which we investigate and provides results on possible shifts in the relevant frequencies or in the strength of comovements over time.¹² Thus, we are able to detect whether the dynamics of correlations and the lead/lag properties may change at different time as well as frequency domains for credit, house price and GDP.

To save space, the specification and estimation result of wavelet analysis are placed in the Appendix B.

As shown in the appendix B, at different time-frequency domains, the wavelet coherence may strengthen or weaken, and the phase difference may change directions for pairwise relations of credit, house price and GDP. We find that the results of wavelet coherence are less decisive, while the phase differences give us a better picture that house prices lead both credit and GDP for most of the time and frequency domains.

To compare the results with the Multivariate STSM, we compute the means of wavelet coherences and phase differences for each time and frequency. We find that the means of wavelet coherence is 0.69 between house price and credit, 0.67 between house price and GDP, and 0.68 between credit and GDP. It turns out that the means of wavelet coherences for all pairwise variables are consistent with the results of Multivariate STSM in Table 3, where house price and credit have highest coherence, followed by the coherence between credit and GDP, and finally by house price and GDP.

¹²For more details about the wavelet analysis, see Hanus and Vacha (2020), Torrence and Compo (1998), and Grinsted et al. (2004).

Furthermore, the mean of phase difference is 0.43 between house price and credit, 0.17 between house price and GDP, and -0.24 between credit and GDP. The results are also consistent with the findings from our Multivariate STSM in Table 3, where house price cycles lead both credit and GDP cycles, and GDP leads credit cycles.

6 Identification of Upturns and Downturns of Financial Cycles

We are now ready to study the possible factors that explain the dynamics of financial cycles in Taiwan. For this purpose, in this section we identify the upturns and downturns of financial cycles. In the next section, we use machine learning to select the best macroeconomic variables that predict the downturns of the financial cycles in Taiwan.

Given the estimated financial cycles from the multivariate STSM, we identify the periods of upturns (troughs to peaks) and downturns (peaks to troughs) using the method by Harding and Pagan (2002).¹³ Table 5 lists the ranges of periods from trough to peak as well as from peak to trough for these two variables. The upturns and downturns of house price and credit cycles are depicted in Figure 2, where the shaded areas represent periods of downturns. There are four downturns for the house price cycle. The first three downturns are roughly associated with the Asian financial crisis, global financial crisis, European sovereign debt crisis, respectively. The last one occurred when the effect of macroprudential measures taken by Taiwan's central bank (mainly restrictions on LTV) kicked in.

We find that the average amplitudes of upturns and downturns are larger for house prices (2.8 and 2.8) than for credit (2.6 and 2.4). As for duration of both house prices and credit cycles, downturns (14.2 and 13.8 quarters) last longer than upturns (10.3 and 9.3 quarters). Finally, the total duration of house price cycles (24.5 quarters) is larger than that of credit cycles (23.1 quarters).

¹³Note that we use the package of Business Cycle Dating (BCDating) in R, specifying the minimum length of a cycle and minimum length of a phase of a cycle so that the duration of a complete cycle is close to the average length of cycles identified by the multivariate STSM from last section.

[Figure 2 inserted here]

Table 5a Identification of Upturns and Downturns of House Price Cycles

	Upturn (Trough to Peak)	Downturn (Peak to Trough)
1	1994Q2 – 1994Q4	1995Q1 – 2000Q4
2	2001Q1 – 2004Q4	2005Q1 – 2008Q4
3	2009Q1 – 2010Q4	2011Q1 – 2012Q1
4	2012Q2 – 2013Q4	2014Q1 – 2016Q4
5	2017Q1 – 2017Q3	
<hr/>		
Amplitude (%)	2.8	2.8
<hr/>		
Duration (Quarters)	10.3	14.2

Note: the amplitude measures the average decline (increase) in the level of house price cycle from peak (trough) to trough (peak).

Table 5b Identification of Upturns and Downturns of Credit Cycles

	Upturn (Trough to Peak)	Downturn (Peak to Trough)
1	1994Q2 – 1995Q3	1995Q4 – 1997Q3
2	1997Q4 – 1998Q4	1999Q1 – 2002Q4
3	2003Q1 – 2006Q4	2007Q1 – 2009Q4
4	2010Q1 – 2011Q3	2011Q4 – 2016Q2
5	2016Q3 – 2017Q3	
<hr/>		
Amplitude (%)	2.6	2.4
<hr/>		
Duration (Quarters)	9.3	13.8

Note: the amplitude measures the average decline (increase) in the level of credit cycle from peak (trough) to trough (peak).

7 Machine Learning

Based on the identified upturns and downturns in Table 5, let the dummy q_t^j indicates the periods of downturn or upturn for a financial cycle, with j being either house prices

or credit:

$$q_t^j = \begin{cases} 1, & \text{when time } t \text{ is in downturn (peaks to troughs),} \\ 0, & \text{when time } t \text{ is in upturn (troughs to peaks).} \end{cases}$$

We first follow the conventional method by using the single-variable logistic regression to fit the probability of a financial downturn. To save space, the results are not reported here, but are available upon request. The problem of a single-variable logistic regression is that it uses very limited information and fails to incorporate other useful macroeconomic variables to explain changes in house prices or credit cycles. Even though it is desirable to include as many variables as possible, however, the loss of degrees of freedom can be substantial and the logistic regression can be sensitive to collinearity among explanatory variables.

To allow for making use of more data without losing power and precision of the analysis, we apply the approach of machine learning to evaluate the importance of a macroeconomic variable for fitting the downturns of financial cycles. Two types of machine learning algorithms are used – random forest and boosting. As discussed in Section 2, the two algorithms are able to deal with a large number of variables.

We describe the specifications of two machine learning approaches in Appendix C. To evaluate the importance of a macroeconomic variable in fitting the downturns of financial cycles under random forest, we follow Breiman (2001) in using the measure Mean Decrease Gini (MDG) or GINI Importance. A variable is more important relative to others if the metric is larger. As for boosting, we use the measure Relative Influence (RI), which randomly permutes each predictor variable at a time and computes the associated reduction in predictive performance, similar to GINI Importance that Breiman (2001) uses for random forest. The metrics for evaluating the relative importance of a variable, MDG and RI, are covered in the Appendix C.

To compare the performance of these two algorithms, we consider three criteria. The first metric evaluates a model’s performance in classification. The other two measures are related to a model’s performance in predicting the probability of downturns, particularly for the out-of-sample forecasting.

First, we use AUROC which measures the area under the receiver operating characteristic (ROC) curve and 45 degree line. It is used to evaluate a model’s performance in

classification. The value of AUROC is between 0.5 and 1. The performance of a model is better when its AUROC is closer to 1.

Second, we use the quadratic probability score (*QPS*) to evaluate the forecasting power of the model, defined as the mean square errors of model prediction:

$$QPS = \frac{1}{T-h} \sum_t^{T-h} (\hat{q}_{t+h} - q_{t+h})^2,$$

where q_t is a binary variable indicating an upturn or downturn (0 or 1), while \hat{q}_t is the predicted probability of the model. The metric *QPS* is between 0 and 1. The forecasting power of the model is better if *QPS* is closer to zero.

Third, in addition to *QPS*, we also consider the log probability score (*LPS*), which is defined as

$$LPS = -\frac{1}{T-h} \sum_t^{T-h} [q_{t+h} \ln(\hat{q}_{t+h}) + (1 - q_{t+h}) q_{t+h} \ln(1 - \hat{q}_{t+h})].$$

Note that *LPS* can be between 0 and ∞ . The forecasting power of the model is better if *LPS* is closer to zero.

7.1 Parameter Value Selection for Machine Learning

7.1.1 Random forest

We use k-fold cross validation for model evaluation, where k is set to be 5. Following Breiman (2001), the number of variables randomly sampled as candidates at each split is set to be \sqrt{J} , where J is the number of variables. Also, the lowest number of observations at the terminal node is chosen to be 1.¹⁴

Next, we describe how to reduce the size of decision trees by pruning to raise efficiency and prediction performance. Firstly, we consider the house price cycles. To obtain the optimal number of in-sample decision trees, we set the number decision trees to be 3000

¹⁴For selecting the number of variables randomly sampled, Breiman (2001) suggests trying the default number \sqrt{J} , half of the default, and twice the default, and pick the best. Liaw and Wiener (2002) point out the results generally do not change dramatically. Even with the number set to be 1, it can generate very good performance for some data.

initially. We then compute the OOB (out-of-bag) error rates, which are the average errors for each observation calculated using predictions from the trees that do not contain the training observation in their respective bootstrap sample. The resulting plot of the OOB error rates allows us to approximate a suitable value of decision trees at which the error stabilizes.

From Figure 3a, the error rate for those being actually downturns (labelled as 1) declines and stabilizes at around 10% (green line), as the number of decision trees grows. On the other hand, the error rate for those being actually upturns (labelled as 0) stabilizes at around 57% (red line), as the number of decision trees rises. The OOB error rate (black line) declines as the number of decision trees increases, and becomes stable at around 29%. As a result, the optimal number of decision trees is set to be 300, at which the OOB error rate is stabilized. Thus, the optimal number of in-sample decision trees for house price cycles is set to be 300, and similarly the out-of-sample decision trees for house price cycles is also set to be the same number.¹⁵

Using the same procedure to choose the optimal decision trees for credit cycles. Figure 3b shows that the number of 400 decision trees allows the estimates of OOB error rate (black line) to stabilize. Thus, we set the numbers of both in-sample and out-of-sample decision trees for credit cycles to be 400.

7.1.2 Boosting

In general, the performance of fit accuracy improves as the number of boosting iterations increased. However, it may lead to the problem of overfitting. We need to find the least number of iterations which is sufficient to build a model that generalizes well to unseen data.

We follow Ridgeway (2012) by specifying the loss function be Bernoulli distribution (logistic regression for 0-1 outcomes), and then set the shrinkage parameter to be 0.005, cross validation fold to be 5, upper limit of iteration to be 20,000, and finally the tree

¹⁵Usually, a large number of trees are necessary to get stable estimates of variable importance. However, Liaw and Wiener (2002) suggests that even though the variable importance measures may vary for each run of iteration, the ranking of variable importance is quite stable.

depth is set to be 1, as in Friedman et al. (2001).

As for the number of iteration for boosting, we use the cross validation to determine the optimal number of iteration for the algorithm. Using the function `gbm.perf` built in R package, we extract the optimal number of iterations using cross-validation. The number of iteration turns out to be larger than the default in R package (i.e., 100), it is selected to be the optimal number of iteration, otherwise, it is set to be the default number 100. The reason is that, as Pan and Bai (2015) points out, boosting with too few iterations will not be able to capture important features of the data.

Taking the house price cycles in-sample fitting as an example. In Figure 3c, the black line is the training bernoulli deviance, the green line is the testing bernoulli deviance. The number of iteration selected for prediction is the number that minimizes the testing bernoulli deviance on the cross-validation folds. We can see that testing bernoulli deviance (in green) is minimized when the number of iteration reaches 650, which is set to be the optimal number of iteration for house price cycles. Following the same procedure, the optimal number of iteration for credit cycles is 100.

[Figure 3 here]

7.2 In-Sample Fitting

Table 6a and 6b show the relative importance of top 12 macro variables out of 74 variables in explaining the downturns of house prices and credit, respectively. Given the measure of AUROC, random forest performs better than boosting in explaining downturns of credit cycles.

From Table 6a, both algorithms suggest that Taiwan's house price downturns are mainly affected by domestic factors such as building permits, bank loans, M1B, core CPI, CPI, electricity consumption, major financial institutions deposits, and foreign factor such as China's industrial production index. Other important macroeconomic variables explaining the downturns of house prices include regular earnings of industrial and service sectors, imports of machineries & electrical equipment, 1-90 day NCD, loan rates, and also OECD composite leading indicator and US PMI.

Note that high explanatory power of core CPI and CPI may suggest the importance of inflation hedging motives in housing demand, while the importance of China's industrial production index reflect the close ties in trades and financial interdependence with China, which may affect housing demand by way of changing exports and household incomes. In summary, this suggests that not only changes in domestic monetary policy and economic fundamentals, but also economic outlooks of China are important in explaining the likelihood of house price downturns.

From Table 6b, the top domestic macroeconomic variables selected by both algorithms that explain the downturns of credit cycles include overnight interbank rates, commercial paper rate, unemployment rate, employment, and WPI. As for foreign factors affecting Taiwan's credit cycles, both algorithms choose the federal funds rate and US term spread. Note that US term spread represents the changes in economic outlook and monetary policy, and has been considered a very important indicator for predicting US recessions. Other important macroeconomic variables also include NCD rates, M2, manufacturing inventory values, Taiwan's leading indicator, and foreign factors such as US IP index. Summing up, Taiwan's credit cycles are not only influenced by domestic business outlook in general, but also substantially influenced by US monetary policy and term spread.

[Table 6a, 6b here]

7.3 Out-of-Sample Forecasting

Given in-sample model fitting, we then use rolling window out-of-sample forecasting to perform h -period ahead out-of-sample prediction for the likelihood of financial cycles downturns.

7.3.1 Rolling Window Out-of-Sample Forecasting

The procedure for rolling window out-of-sample forecasting is as follows. First, we fit the model using in-sample data from 1995Q2 to 2004Q4, and then substitute the data point 2005Q1 into the model to perform h -period ahead forecasting for the financial

cycle downturns, where $h = 1, 2, 3, 4$. Thus, we obtain the probabilities of financial cycle downturns for 2005Q2, 2005Q3, 2005Q4, and 2006Q1.

Next, we move forward to the next rolling window by adding an additional data point 2005Q1 and deleting the initial data point 1995Q2. Now the model is fitted using in-sample data from 1995Q3 to 2005Q1. Combined with the newly estimated parameter values, we substitute the data point 2005Q2 to estimate the probabilities of financial cycle downturns for the next 4 quarters. The procedure is repeated till the end of sample period, 2017Q3.

7.3.2 Evaluating Performance of Out-of-Sample Forecasting

The out-of-sample forecasting of the two approaches are evaluated using the metrics QPS, LPS and AUROC, respectively. The results are listed in Table 7a and 7b for house price cycles and credit cycles, respectively. The metrics that performs better are marked in bold.

From Table 7a, all the values of QPS and LPS of random forest are lower than those of boosting, and all the values of AUROC of random forest are higher than those of boosting. This indicate that random forests performs better than boosting at all forecasting horizons for house price cycles. Similarly, from Table 7b all the metrics of QPS, LPS, and AUROC shows that random forest performs better than boosting at all forecasting horizons for credit cycles.

One possible explanation why in general boosting performs worse than other ensemble learning is that, as Long and Servedio (2009) point out, boosting is highly susceptible to random classification noise.

7.3.3 Relative Importance of a Macro Variable

Table 8a and 8b show the relative importance of top 12 macroeconomic variables in out-of-sample forecasting the downturns of house prices and credit, respectively, using random forest and boosting. We find that all top 12 important variables in Table 6a and 6b for in-sample fitting are almost all included in Table 8a and 8b for out-of-sample forecasting horizon $h = 1$ to 4, except the orderings are somewhat different.

As for the foreign factors affecting Taiwan’s house price cycles, the difference from in-sample fitting is that China’s industrial production index is no longer important for out-of-sample forecasting; instead, the federal funds rate becomes important for predicting Taiwan’s house price cycles. Also, at forecasting horizon $h = 3$ and $h = 4$, the choices of both machine learning approaches match those of in-sample fitting in selecting OECD leading indicators as an important foreign macro variable for predicting downturns of house price cycles. Notably, the importance of foreign macro variables rises as the forecasting horizon increases.

Similarly, as for credit cycles, almost all of the important macro variables selected by the two machine learning approaches for in-sample fitting Taiwan’s credit cycles in Table 6b are covered in the out-of-sample forecasting in Table 8b. In particular, both random forest and boosting choose federal funds rate, OECD composite leading indicator (CLI), US term spread, and major Asian leading indicators as the leading foreign macro variables in predicting Taiwan’s credit cycles. Summarizing results from in-sample fitting and out-of-sample forecasting, we find that Taiwan’s financial cycles are deeply affected by fluctuations in international financial and economic conditions.¹⁶

Finally, as a robustness check, given the top 12 macro variables that are important for out-of-sample forecasting chosen by machine learning, we test the out-of-sample forecasting power of these 12 macro variables. The results are listed in Table 9a and 9b. Compare Table 9 with Table 7, we find that the out-of-sample forecasting power of these 12 macro variables performs better in predicting Taiwan’s financial cycle downturns than that using all macro variables under most of the evaluation metrics, QPS, LPS, and AUROC. This means that the variable ranking of relative importance based on machine learning is a reliable result.

¹⁶Note that China’s industrial production index matters only in the in-sample fitting, but not in out-of-sample forecasting. A possible explanation is that Taiwan’s manufacturers take orders but mainly produce in China for exports. Since exogenous shocks from advanced economies affect both Taiwan and China, the predicting power of China’s industrial production index is weakened in the out-of-sample forecasting, compared to OECD’s leading indicators or US monetary policy.

8 Concluding Remarks

In this paper, we study the characteristics of financial cycles (credit and house prices) and their interactions with business cycles in Taiwan. We find evidence that Taiwan's financial cycles have lower frequencies than business cycles and that house price cycles lead both credit and business cycles, however, the length of financial cycles in Taiwan is substantially shorter than those estimated using data from industrialized economies, similar to findings in Pontines (2017) for other east Asian economies. This remains an intriguing question worth pursuing in the future. We also find that credit and house price cycles have a higher correlation than other pairs, and that house price cycles lead both credit and GDP cycles.

When we use both approaches of machine learning to evaluate the importance of a macroeconomic variable for in-sample fitting and out-of-sample forecasting the downturns of financial cycles, the top chosen macroeconomic variables suggest that Taiwan's financial cycles are deeply affected by exogenous shocks from foreign economies, reflecting Taiwan's close linkage in trades and financial interdependence with other countries such as China, as well as spillover effect from the Fed's monetary policy.

The financial cycles have played a more and more important role in the current debate on how to raise resilience of the financial system. An important policy implication is that to foster financial stability financial supervisors need to monitor the medium-term risk of financial cycle, other than containing short-term fluctuations of business cycles. This is because financial vulnerabilities take some time to develop, and thus there is a considerable time lag before financial supervisors are able to identify potential systemic risk. Moreover, factors and channels that affect financial cycles, as identified earlier, can be different from those affecting business cycles. As a result, instruments of macroprudential policies are suitable for monitoring and managing the medium-term risk of financial cycles, which have been extensively adopted by financial supervisors around the globe. Our results from machine learning that study the driving forces of financial cycles can help selecting the appropriate instrument for a small open economy such as Taiwan.

Finally, existing theoretical models tend to add various financial frictions into an otherwise standard equilibrium macroeconomic models. However, the financial cycles may

generate, rather than simply propagate shocks, and their interactions with the business cycles may be more complicated than assumed in existing papers. The evidence presented here can also help develop an analytical framework incorporating the medium-term financial cycles alongside with the business cycles in a general equilibrium models for policy evaluations.

References

- [1] Aikman, D., A. Haldane, and B. Nelson (2015), “Curbing the credit cycle,” *The Economic Journal*, 125, 1072-1109.
- [2] Berge, T. (2015), “Predicting recessions with leading indicators: model averaging and selection over the business cycle,” *Journal of Forecasting*, 34(6), 455-471.
- [3] Bordo, Michael D. and Joseph G. Haubrich (2010), “Credit crises, money and contractions: an historical view,” *Journal of Monetary Economics*, 57, 1-18.
- [4] Borio, Claudio (2014), “The financial cycle and macroeconomics: What have we learnt?” *Journal of Banking & Finance*, Elsevier, 45(C), 182-198.
- [5] Breiman, Leo (2001), “Random forests,” *Machine Learning*, 45(1), 5–32.
- [6] Brock, W. A., W. D. Dechert, J. A. Scheinkman, and B. LeBaron (1996), “A test for independence based on the correlation dimension,” *Econometric Reviews*, 15, 197-235.
- [7] Chen, Nan-Kuang (2001), “Bank net worth, asset prices and economic activity,” *Journal of Monetary Economics*, 48, 415-436.
- [8] Chen, X., A. Kontonikas, and A. Montagnoli (2012), “Asset prices, credit and the business cycle,” *Economic Letters*, 117, 857–861.

- [9] Claessens, Stijn, M. Ayhan Kose, and Marco E. Terrones (2011), “Financial cycles: what? how? when?” In NBER International Seminar on Macroeconomics 2010, edited by Richard Clarida and Francesco Giavazzi, 303–43, Chicago: University of Chicago Press.
- [10] Claessens, Stijn, M. Ayhan Kose, and Marco E. Terrones (2012), “How do business and financial cycles interact?” *Journal of International Economics*, 87(1), 178-190.
- [11] Dell’Ariccia, Giovanni, Deniz Igan and, Luc A. Laeven (2008), “Credit booms and lending standards: evidence from the subprime mortgage market,” manuscript.
- [12] Drehmann, M., C. Borio and K. Tsatsaronis (2012), “Characterising the financial cycle: don’t lose sight of the medium term!” BIS Working Papers, no 380, June.
- [13] Duca, John V., John Muellbauer and Anthony Murphy (2010), “Housing markets and the financial crisis of 2007–2009: lessons for the future,” *Journal of Financial Stability* 6, 203–17.
- [14] Duca, John V., John Muellbauer and Anthony Murphy (2011), “Shifting credit standards and the boom and bust in US house prices,” CEPR discussion paper 8361, CEPR: London.
- [15] Friedman, Jerome, Trevor Hastie, and Robert Tibshirani. (2001), *The elements of statistical learning*. Vol. 1. Springer Series in Statistics New York, NY, USA.
- [16] Friedman, J. H. (2001), “Greedy function approximation: A gradient boosting machine,” *Annals of Statistics*, 29(5), 1189-1232.
- [17] Friedman, J.H. and T. Hastie (2000), “Additive logistic regression: a statistical view of boosting,” *Annals of Statistics*, 28(2), 337–407.
- [18] Grinsted, A., J.C. Moore, and S. Jevrejeva (2004), “Application of the cross wavelet transform and wavelet coherence to geophysical time series,” *Nonlinear Processes in Geophysics*, 11(5/6), 561–566.

- [19] Hanus, L. and L. Vacha (2020), “Growth cycle synchronization of the Visegrad Four and the European Union,” *Empirical Economics*, 58, 1779–1795.
- [20] Harding, D. and A.R. Pagan (2002), “Dissecting the cycle: a methodological investigation,” *Journal of Monetary Economics*, 49(2), 365-381.
- [21] Harvey, A. C. and S. J. Koopman (1997), Multivariate structural time series models, in Heij, C., H. Schumacher, and B. Hanzon (Eds.), *System Dynamics in Economic and Financial Models*, 269-298, New York, NY: Wiley.
- [22] Iacoviello, Matteo (2005), “House prices, borrowing constraints and monetary policy in the business cycle,” *American Economic Review*, 95(3), 739-764.
- [23] Jorda, O., M. Schularick, and A. Taylor (2013), “When credit bites back: leverage, business cycles, and crises,” *Journal of Money Credit and Banking*, 45(s2), 3-28.
- [24] Kiyotaki, N. and J. Moore (1997), “Credit cycles,” *Journal of Political Economy*, 105(2), 211–48.
- [25] Koopman, Siem Jan and Andre Lucas (2005), “Business and default cycles for credit risk,” *Journal of Applied Econometrics*, 20(2), 311-323.
- [26] Long, P.M., and R.A. Servedio (2009), “Random classification noise defeats all convex potential boosters,” *Machine Learning*, 78(3), 287–304.
- [27] Liaw, Andy and Matthew Wiener (2002), “Classification and regression by random forest,” *R News*, 2, 18-22.
- [28] Lilliefors, H. W. (1967), “On the Kolmogorov-Smirnov test for normality with mean and variance unknown,” *Journal of the American Statistical Association*, 62, 399-402.
- [29] Mian, Atif R. and Amir Sufi (2009), “The consequences of mortgage credit expansion: evidence from the U.S. mortgage default crisis,” *Quarterly Journal of Economics*, 124, 1449-1496.
- [30] Miranda-Agrippino, Silvia and Helene Rey (2019), “US monetary policy and the global financial cycle,” Working paper.

- [31] Mishkin, F.S. (2008), “How should we respond to asset price bubbles?” Speech at the Wharton Financial Institutions Center, Philadelphia.
- [32] Murray, C. J. (2003), “Cyclical properties of Baxter-King filtered time series,” *Review of Economics and Statistics*, 85(2), 472–476.
- [33] Pan, Wei and Haiyan Bai (2015), *Propensity score analysis: fundamentals and developments*, Guilford Publications.
- [34] Pontines, Victor (2017), “The financial cycles in four East Asian economies,” *Economic Modelling*, 65, 51-66.
- [35] Raffinot, Thomas (2017), “Investing through economic cycles with ensemble machine learning algorithms,” Working paper.
- [36] Rand, John and Finn Tarp (2002), ”Business cycles in developing countries: are they different?,” *World Development*, 30(12), 2071–2088.
- [37] Reinhart, Carmen M. and Kenneth S. Rogoff (2009), *This time is different: eight centuries of financial folly*, Princeton University Press, Princeton, N.J..
- [38] Rey, Helene (2013), “Dilemma not trilemma: The global financial cycle and monetary policy independence”, Jackson Hole conference proceedings, Kansas City Fed, 2013.
- [39] Ridgeway, G. (2012), “Generalized boosted models: a guide to the gbm package,” Working paper.
- [40] Runstler, Gerhard (2004), “Modelling phase shifts among stochastic cycles,” *Econometrics Journal*, 7(1), 232-248.
- [41] Runstler, Gerhard and Marente Vlekke (2018), “Business, housing, and credit cycles,” *Applied Econometrics*, 33, 212-226.
- [42] Schapire, Robert E. (1999), “A brief introduction to boosting,” *Proceedings of the Sixteenth International Joint Conference on Artificial Intelligence*, 1-6.

- [43] Schularick, Moritz and Alan M. Taylor (2012), “Credit booms gone bust: monetary policy, leverage cycles, and financial crises, 1870–2008,” *American Economic Review*, 102(2), 1029-10.
- [44] Schuler, Yves Stephan, Paul Hiebert and Tuomas A. Peltonen (2015), “Characterizing financial cycles across europe: one size does not fit all,” ECB working paper 1846.
- [45] Thode Jr., H.C. (2002), *Testing for normality*, Marcel Dekker, New York.
- [46] Torrence, C. and G.P. Compo (1998), “A practical guide to wavelet analysis,” *Bulletin of the American Meteorological Society*, 79(1), 61–78.

Table 6a Ordering of Macro Variables Based on Machine Learning -- House Prices

Random Forest		Boosting	
Variable	MDG	Variable	RI
building permits	2.152	building permits	22.09
loans of major monetary institutions	1.055	core CPI	9.46
core CPI	0.778	real M1B	7.65
real M1B	0.72	loans of major monetary institutions	5.94
M1B	0.653	total electricity consumption	4.88
CPI	0.578	China's industrial production index	4.82
OECD composite leading indicator (CLI)	0.471	major financial institutions deposits	2.73
total electricity consumption	0.455	1-90 day NCD	2.70
major financial institutions deposits	0.436	CPI	2.57
regular earnings of industrial and service sectors	0.436	loan rate of new lending by 5 major banks	2.53
US PMI	0.420	currency in circulation	2.25
China's industrial production index	0.397	imports of machineries & electrical equipment	2.11
AUROC	0.83	AUROC	0.96

Note: To select the best available split for Random Forest, mean decrease gini (MDG) or GINI importance measures the average gain of purity by splits of a given variable. The measure adds up the weighted impurity decreases for all nodes where the macroeconomic variable is used and is then averaged over the sample decision trees in the forest. The larger the metric, the more importance the variable is. As for Boosting, we use the measure relative influence (RI), which randomly permutes each predictor variable at a time and computes the associated reduction in predictive performance, similar to GINI importance measures Breiman (2001) uses for Random Forest.

Table 6b Ordering of Macro Variables Based on Machine Learning -- Credit

Random Forest		Boosting	
Variable	MDG	Variable	RI
non-agricultural employment	1.44	unemployment rate	19.30
overnight interbank rates	1.41	overnight interbank rates	11.61
unemployment rate	1.37	non-agricultural employment	8.61
1-30 day commercial paper rate	1.31	US term spread	7.41
regular employment of industrial and service sectors	1.13	WPI	7.19
1-90 day NCD	1.13	regular employment of industrial and service sectors	4.55
31-90 day commercial paper rate	1.10	1-30 day commercial paper rate	4.54
WPI	1.05	feral funds rate	4.20
feral funds rate	1.02	manufacturing inventory value	4.03
US term spread	0.98	currency in circulation	3.96
composite index of contemporary indicators	0.79	M2	3.07
US industrial production index	0.77	Taiwan's leading indicator	2.49
AUROC	1.00	AUROC	0.85

Note: See Table 6a.

Table 7a Evaluation Metrics of Out-of-Sample Forecasting for House Price Cycles

		Forecasting horizon			
		$h = 1$	$h = 2$	$h = 3$	$h = 4$
Random Forest	QPS	0.196	0.183	0.188	0.170
	LPS	0.577	0.546	0.557	0.513
	AUROC	0.764	0.798	0.757	0.822
Boosting	QPS	0.224	0.204	0.227	0.174
	LPS	0.641	0.604	0.675	0.526
	AUROC	0.665	0.681	0.606	0.780

Table 7b Evaluation Metrics of Out-of-Sample Forecasting for Credit Cycles

		Forecasting horizon			
		$h = 1$	$h = 2$	$h = 3$	$h = 4$
Random Forest	QPS	0.204	0.208	0.205	0.214
	LPS	0.610	0.606	0.635	0.633
	AUROC	0.720	0.694	0.717	0.692
Boosting	QPS	0.224	0.214	0.230	0.226
	LPS	0.660	0.628	0.679	0.646
	AUROC	0.663	0.684	0.625	0.649

Table 8a Relative Importance of Top 12 Macroeconomic Variables for House Price Cycles

Rank	Random Forest				Boosting			
	<i>h</i> =1	<i>h</i> =2	<i>h</i> =3	<i>h</i> =4	<i>h</i> =1	<i>h</i> =2	<i>h</i> =3	<i>h</i> =4
1	loan rate of new lending by 5 major banks	loan rate of new lending by 5 major banks	loan rate of new lending by 5 major banks	OECD composite leading indicator (CLI)	loan rate of new lending by 5 major banks	loan rate of new lending by 5 major banks	loan rate of new lending by 5 major banks	OECD composite leading indicator (CLI)
2	regular employment of industrial and service sectors	regular employment of industrial and service sectors	overnight interbank rates	OECD composite leading indicators(OECD + Major Six NME)	building permits	regular employment of industrial and service sectors	overnight interbank rates	regular earnings of industrial and service sectors
3	core CPI	unemployment rate	import quantity index	31-90 day commercial paper rate	core CPI	feral funds rate	OECD composite leading indicator (CLI)	loans and investment of all monetary institutions
4	building permits	overnight interbank rates	31-90 day commercial paper rate	loans and investment of major financial institutions	feral funds rate	regular earnings of industrial and service sectors	loans and investment of all monetary institutions	loan rate of new lending by 5 major banks
5	31-90 day commercial paper rate	31-90 day commercial paper rate	OECD composite leading indicator (CLI)	loans and investment of all monetary institutions	regular employment of industrial and service sectors	unemployment rate	unemployment rate	overnight interbank rates
6	unemployment rate	feral funds rate	1-90 day NCD	regular earnings of industrial and service sectors	unemployment rate	overnight interbank rates	feral funds rate	31-90 day commercial paper rate
7	M1B	1-90 day NCD	advanced country industrial production index	overnight interbank rates	regular earnings of industrial and service sectors	building permits	regular employment of industrial and service sectors	composite index of contemporary indicators
8	1-90 day NCD	core CPI	regular employment of industrial and service sectors	loan rate of new lending by 5 major banks	imports of machineries & electrical equipment	core CPI	regular earnings of industrial and service sectors	US industrial production index
9	regular earnings of industrial and service sectors	regular earnings of industrial and service sectors	unemployment rate	composite index of contemporary indicators	M1B	loans and investment of all monetary institutions	advanced country industrial production index	feral funds rate
10	feral funds rate	M1B	1-30 day commercial paper rate	advanced country industrial production index	WPI	US industrial production index	real import value	Asia-Pacific industrial production index
11	overnight interbank rates	loans of major monetary institutions	loans of major monetary institutions	loans of major monetary institutions	currency in circulation	loans of major monetary institutions	1-30 day commercial paper rate	loans of major monetary institutions
12	loans of major monetary institutions	building permits	loans and investment of all monetary institutions	feral funds rate	overnight interbank rates	M1B	Asia-Pacific industrial production index	core CPI

Table 8b Relative Importance of Top 12 Macroeconomic Variables for Credit Cycles

<i>h</i> -ahead Rank	Random Forest				Boosting			
	<i>h</i> =1	<i>h</i> =2	<i>h</i> =3	<i>h</i> =4	<i>h</i> =1	<i>h</i> =2	<i>h</i> =3	<i>h</i> =4
1	unemployment rate	unemployment rate	feral funds rate	currency in circulation	unemployment rate	feral funds rate	feral funds rate	currency in circulation
2	feral funds rate	feral funds rate	unemployment rate	unemployment rate	feral funds rate	currency in circulation	unemployment rate	building permits
3	regular employment of industrial and service sectors	31-90 day commercial paper rate	OECD composite leading indicator (CLI)	building permits	currency in circulation	unemployment rate	currency in circulation	unemployment rate
4	non-agricultural employment	currency in circulation	currency in circulation	feral funds rate	non-agricultural employment	31-90 day commercial paper rate	OECD composite leading indicator (CLI)	feral funds rate
5	1-30 day commercial paper rate	regular employment of industrial and service sectors	regular employment of industrial and service sectors	M1B	US term spread	building permits	building permits	imports of machineries & electrical equipment
6	31-90 day commercial paper rate	building permits	building permits	real M1B	31-90 day commercial paper rate	regular employment of industrial and service sectors	imports of machineries & electrical equipment	index of industrial labor productivity
7	currency in circulation	OECD composite leading indicator (CLI)	imports of machineries & electrical equipment	imports of machineries & electrical equipment	regular employment of industrial and service sectors	US term spread	regular employment of industrial and service sectors	loan rate of new lending by 5 major banks
8	overnight interbank rates	major five Asia leading indicators	US term spread	US term spread	1-30 day commercial paper rate	major five Asia leading indicators	US term spread	US term spread
9	US term spread	1-30 day commercial paper rate	31-90 day commercial paper rate	regular employment of industrial and service sectors	REER	OECD composite leading indicator (CLI)	index of industrial labor productivity	real M1B
10	manufacturing unit output labor cost index	US term spread	manufacturing quantity index	export order Index	WPI	index of industrial labor productivity	core CPI	M1B
11	major five Asia leading indicators	production value of manufacturing	industrial production index	31-90 day commercial paper rate	major five Asia leading indicators	REER	31-90 day commercial paper rate	Reserve Money
12	REER	REER	10 years bond rate minus 31-90 day commercial paper rate	10 years bond rate minus 31-90 day commercial paper rate	manufacturing unit output labor cost index	manufacturing unit output labor cost index	WPI	10 years bond rate

Table 9a Evaluation Metrics of Out-of-Sample Forecasting for House Price Cycles

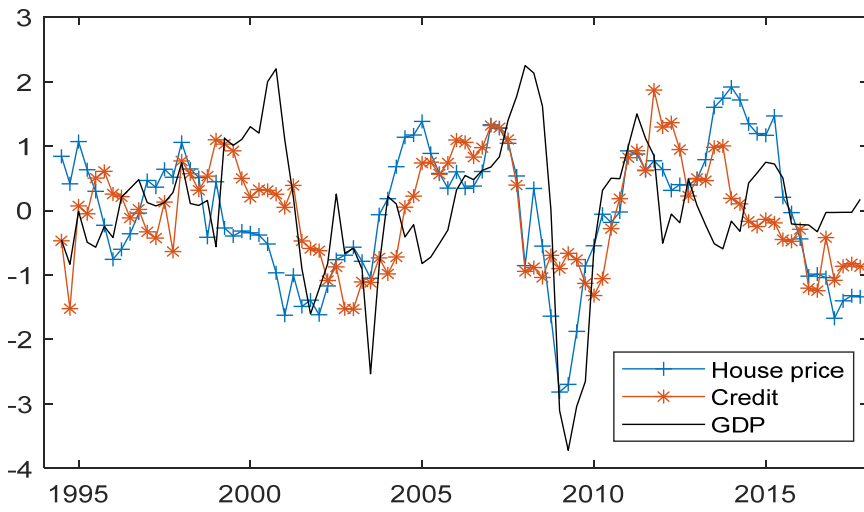
		Forecasting horizon			
		$h = 1$	$h = 2$	$h = 3$	$h = 4$
Random Forest	QPS	0.175	0.158	0.175	0.143
	LPS	0.535	0.492	0.517	0.442
	AUROC	0.828	0.842	0.811	0.858
Boosting	QPS	0.200	0.166	0.181	0.154
	LPS	0.699	0.526	0.547	0.480
	AUROC	0.746	0.819	0.781	0.815

Table 9b Evaluation Metrics of Out-of-Sample Forecasting for Credit Cycles

		Forecasting horizon			
		$h = 1$	$h = 2$	$h = 3$	$h = 4$
Random Forest	QPS	0.176	0.178	0.193	0.191
	LPS	0.597	0.582	0.636	0.579
	AUROC	0.794	0.776	0.730	0.746
Boosting	QPS	0.203	0.190	0.216	0.207
	LPS	0.752	0.562	0.705	0.605
	AUROC	0.734	0.759	0.686	0.706

Figure 1 Estimated Financial and Business Cycles

(a) Multivariate STSM



(b) Financial Cycles Based on Multivariate STSM

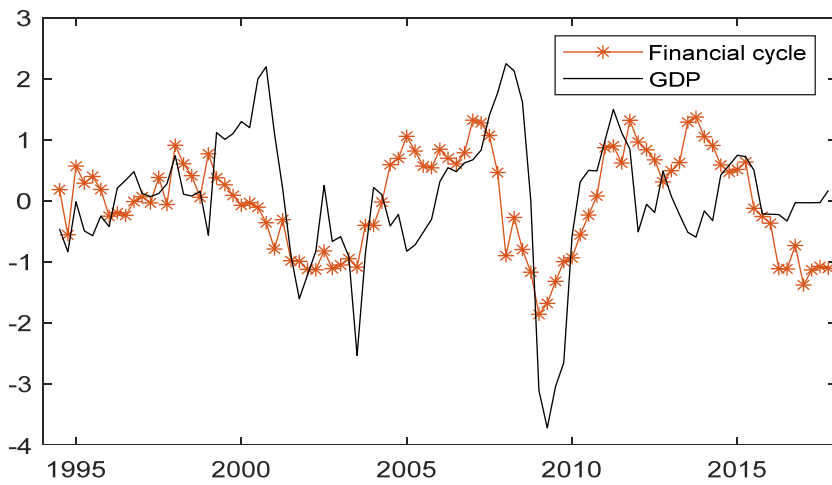
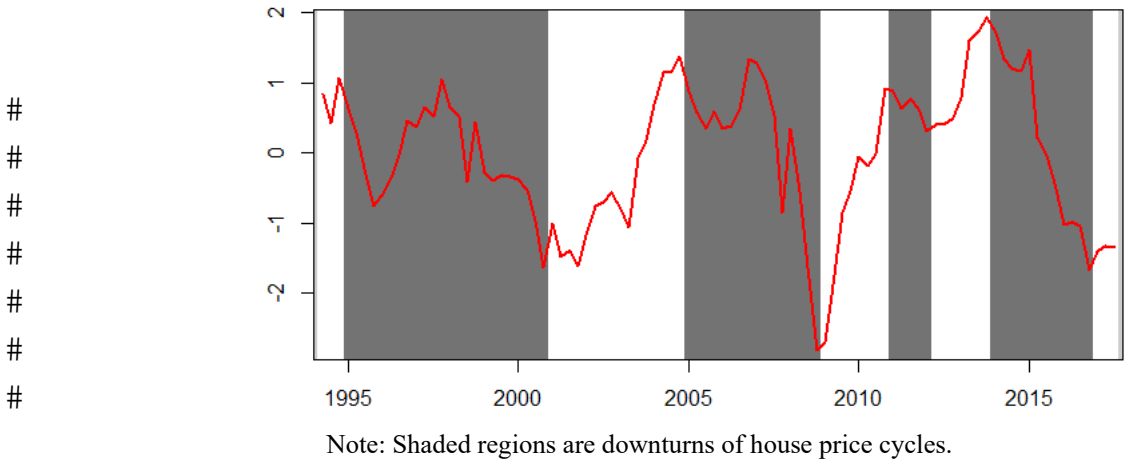
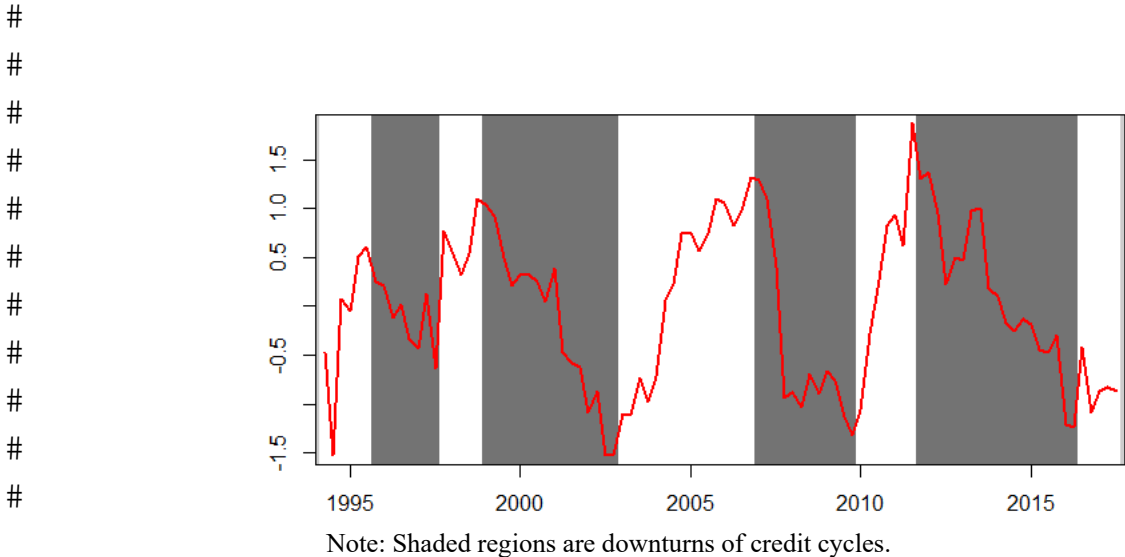


Figure 2a Identification of Upturns and Downturns of House Price Cycles



Note: Shaded regions are downturns of house price cycles.

Figure 2b Identification of Upturns and Downturns of Credit Cycles



Note: Shaded regions are downturns of credit cycles.

#

#

Figure 3a The OOB Error Rate (black line) for Selecting the Number of Decision Trees:
House Price Cycles



Figure 3b The OOB Error Rate (black line) for Selecting the Number of Decision Trees:
Credit Cycles

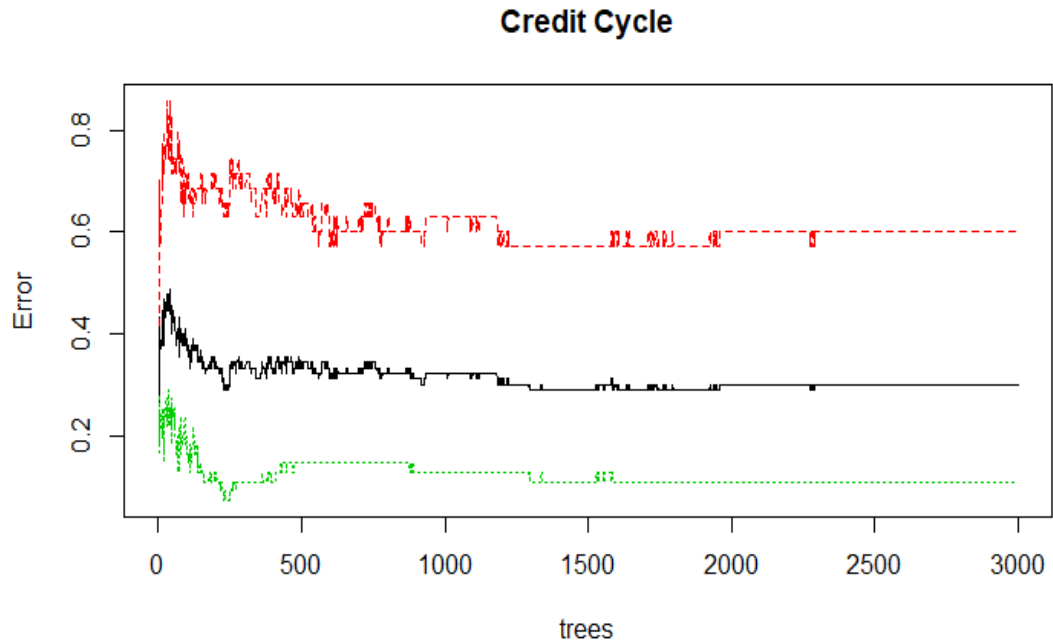
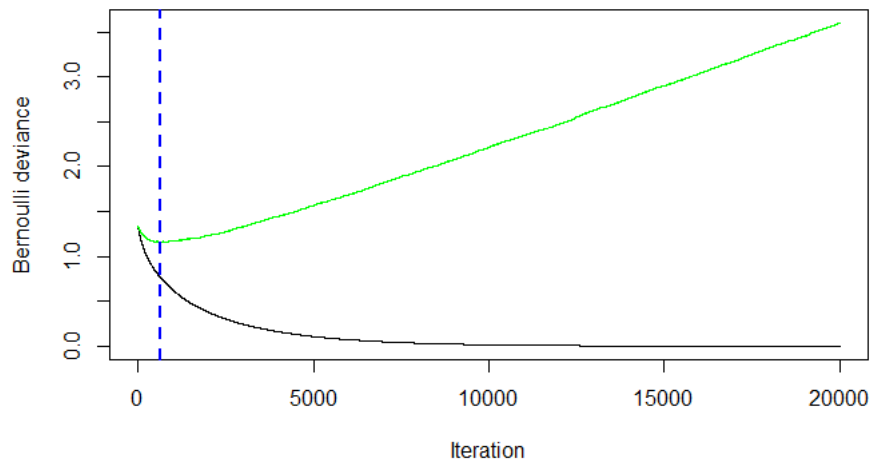


Figure 3c The Testing Bernoulli Deviance for Selecting the Number of Iteration: House Price Cycles



Note: the black line is the training bernoulli deviance, the green line is the testing bernoulli deviance.

#

Appendix

A. Multivariate STSM in State-Space Matrix Form

Define the $2n \times 1$ ($n = 3$) vector $\tilde{\Psi}_t = (\Psi_t, \Psi_t^*)$ with $\Psi_t = (\psi_{1,t}, \psi_{2,t}, \psi_{3,t})'$ and $\Psi_t^* = (\psi_{1,t}^*, \psi_{2,t}^*, \psi_{3,t}^*)'$. Multivariate STSM can be expressed as:

$$\begin{aligned}\mathbf{y}_t &= \boldsymbol{\mu}_t + (B, B^*)\tilde{\Psi}_t + \boldsymbol{\varepsilon}_t, \\ \boldsymbol{\mu}_t &= \boldsymbol{\mu}_{t-1} + \boldsymbol{\beta}_t + \boldsymbol{\eta}_t, \\ \boldsymbol{\beta}_t &= \boldsymbol{\beta}_{t-1} + \mathbf{v}_t,\end{aligned}$$

where $\mathbf{y}_t = (y_{GDP,t}; y_{credit,t}; y_{houseprice,t})'$, $\boldsymbol{\mu}_t = (\mu_{1,t}, \mu_{2,t}, \mu_{3,t})'$ is the trend, $\boldsymbol{\beta}_t = (\beta_{1,t}, \beta_{2,t}, \beta_{3,t})'$ is the slope, the vector $\tilde{\Psi}_t = (\Psi_t, \Psi_t^*)' = (\psi_{1,t}, \psi_{2,t}, \psi_{3,t}, \psi_{1,t}^*, \psi_{2,t}^*, \psi_{3,t}^*)'$ is the stochastic cycle, and $B = (b_{ij})$ and $B^* = (b_{ij}^*)$ are general $n \times n$ matrices.

The $n \times 1$ vector $\boldsymbol{\varepsilon}_t$, the measurement noise in the observations, is normally and independently distributed with mean zero and $n \times n$ covariance matrix Σ_ε , $\boldsymbol{\varepsilon}_t \sim NID(\mathbf{0}, \Sigma_\varepsilon)$. Also, the innovations of trend and slope, $\boldsymbol{\eta}_t$ and \mathbf{v}_t , are also normally and independently distributed with mean zero and covariance matrices, Σ_η and Σ_v , respectively: $\boldsymbol{\eta}_t \sim NID(\mathbf{0}, \Sigma_\eta)$ and $\mathbf{v}_t \sim NID(\mathbf{0}, \Sigma_v)$.

We then rewrite the multivariate STSM in state-space form. The measurement and transition equations are

$$\begin{aligned}\mathbf{y}_t &= \mathbf{P}\boldsymbol{\omega}_t + \boldsymbol{\varepsilon}_t, \quad \boldsymbol{\varepsilon}_t \sim NID(\mathbf{0}, \Sigma_\varepsilon) \\ \boldsymbol{\omega}_t &= \mathbf{Q}\boldsymbol{\omega}_{t-1} + \boldsymbol{\tau}_t, \quad \boldsymbol{\tau}_t \sim NID(\mathbf{0}, \Sigma_\tau)\end{aligned}$$

The state vector $\boldsymbol{\omega}_t$ is given by the $(6n \times 1)$ vector,

$$\boldsymbol{\omega}_t = (\boldsymbol{\mu}_t, \boldsymbol{\beta}_t, \Psi_t, \Psi_t^*, \gamma_t, \gamma_t^*),$$

where the measurement-transition \mathbf{P} matrix can be expressed by

$$\mathbf{P} = [I_3, \mathbf{0}_{3 \times 3}, (B, B^*), \mathbf{0}_{3 \times 3}, \mathbf{0}_{3 \times 3}].$$

Thus, the state transition matrix \mathbf{Q} is given by

$$\mathbf{Q} = \begin{bmatrix} I_3 & I_3 & \mathbf{0}_{3 \times 3} & \mathbf{0}_{3 \times 3} & \mathbf{0}_{3 \times 3} & \mathbf{0}_{3 \times 3} \\ \mathbf{0}_{3 \times 3} & I_3 & \mathbf{0}_{3 \times 3} & \mathbf{0}_{3 \times 3} & \mathbf{0}_{3 \times 3} & \mathbf{0}_{3 \times 3} \\ \mathbf{0}_{3 \times 3} & \mathbf{0}_{3 \times 3} & \mathbf{0}_{3 \times 3} & \mathbf{0}_{3 \times 3} & I_3 & \mathbf{0}_{3 \times 3} \\ \mathbf{0}_{3 \times 3} & \mathbf{0}_{3 \times 3} & \mathbf{0}_{3 \times 3} & \mathbf{0}_{3 \times 3} & \mathbf{0}_{3 \times 3} & I_3 \\ \mathbf{0}_{3 \times 3} & \mathbf{0}_{3 \times 3} & \mathbf{0}_{3 \times 3} & \mathbf{0}_{3 \times 3} & C_\lambda & S_\lambda \\ \mathbf{0}_{3 \times 3} & \mathbf{0}_{3 \times 3} & \mathbf{0}_{3 \times 3} & \mathbf{0}_{3 \times 3} & -S_\lambda & C_\lambda \end{bmatrix},$$

with C_λ and S_λ are $n \times n$ diagonal matrices with elements $C_{\lambda,ii} = \rho_i \cos \lambda_i$ and $S_{\lambda,ii} = \rho_i \sin \lambda_i$ on the main diagonals. The vectors of (γ_t, γ_t^*) represent the original the stochastic cycle. They are auxiliary variables to generate the vector of stochastic cycles (Ψ_t, Ψ_t^*) .

The state-disturbance vector $\boldsymbol{\tau}_t$ is given by

$$\boldsymbol{\tau}_t = \begin{bmatrix} \boldsymbol{\eta}_t \\ \mathbf{v}_t \\ \mathbf{0}_{3 \times 1} \\ \mathbf{0}_{3 \times 1} \\ \boldsymbol{\vartheta}_t^* \\ \boldsymbol{\vartheta}_t \end{bmatrix}$$

where $\boldsymbol{\eta}_t$ represents the trend-disturbances, \mathbf{v}_t are the slope-disturbances. The vector of innovations $\tilde{\boldsymbol{\vartheta}}_t = (\boldsymbol{\vartheta}_t, \boldsymbol{\vartheta}_t^*) = (\vartheta_{1,t}, \vartheta_{2,t}, \vartheta_{3,t}, \vartheta_{1,t}^*, \vartheta_{2,t}^*, \vartheta_{3,t}^*)'$ are the cycle disturbances with covariance matrix $E[\tilde{\boldsymbol{\vartheta}}_t \tilde{\boldsymbol{\vartheta}}_t'] = I_{2n}$.

The model is completed by the assumptions that $\boldsymbol{\varepsilon}_t$, $\boldsymbol{\eta}_t$, \mathbf{v}_t , and $\tilde{\boldsymbol{\vartheta}}_t$ are mutually uncorrelated. The (18×18) disturbance matrix Σ_τ in the transition equation is defined as:

$$\Sigma_\tau = \text{diag}[\Sigma_\eta, \Sigma_v, I_2 \otimes \mathbf{0}_{3 \times 3}, I_{2n}],$$

B. The Wavelet Analysis

The definition of wavelet coherence between two time series, x and y , is as follows,

$$R^2(\tau, s) = \frac{|S(s^{-1}W_{xy}(\tau, s))|^2}{S(s^{-1}|W_x(\tau, s)|^2) \cdot S(s^{-1}|W_y(\tau, s)|^2)}, \quad R^2 \in [0, 1],$$

where $W_x(\tau, s)$ is a wavelet (co-)spectrum, and S is a smoothing function as $S(W) = S_{scale}(S_{time}(W_n(S)))$. Since the estimates of a wavelet power spectrum are sensitive to data at the beginning and at the end, we pad both ends with a sufficient number of zeros to the data. The area affected by zero-padding is denoted the cone of influence (COI).¹

As for the lead/lag relation between two cyclical time series x and y , the phase difference is given by

$$\phi_{x,y} = \tan^{-1} \left(\frac{\Upsilon \{W_{xy}(\tau, s)\}}{\Lambda \{W_{xy}(\tau, s)\}} \right), \quad \text{where } \phi_{x,y} \in [-\pi, \pi],$$

where $\Upsilon \{W_{xy}(\tau, s)\}$ and $\Lambda \{W_{xy}(\tau, s)\}$ are the imaginary and real parts of a cross wavelet transform, respectively. In Figure A1, the phase difference suggests that x leads y when the arrows point to the northeast or southwest, i.e., when $\phi_{x,y}$ is in $[0, \pi/2]$ and $[-\pi, -\pi/2]$; y leads x when the arrows point to northwest or southeast, i.e., when $\phi_{x,y}$ is in $[-\pi/2, 0]$ and $[\pi/2, \pi]$.

In Figure A2-A4 the wavelet coherence of variable x over variable y shows the regions of comovement localized in time-frequency between a pair of time series, x and y , with time on the horizontal axis, while the length of cycles on the vertical axis. Areas in red represent regions with high coherence, while blue color represents lower dependence between the series. The contours with significance level of 5% are also depicted. The significance of the wavelet coherence is obtained using Monte Carlo methods. The regions outside the significant areas indicate no dependence between the series. The white area indicate the cone of influence. The maximum length of cycles we consider is about 8 years. This is a restriction implied by the empirical results.

For convenience, in Figure A2-A4 we also plot the phase differences of x over y in those areas with significant high coherence, indicated by the directions of arrows, which give us lead/lag relation at specific frequency bands.

¹For more details about the wavelet coherence and phase difference, see the Supplementary from Hanus and Vacha (2020), Torrence and Compo (1998) and Grinsted et al. (2004).

As shown in Figure A2, the 3-8 year frequency band has high coherence between house price and credit for most of the sample periods, albeit not entirely significant. Between 2003-2008, however, the coherence of 3-8 year frequency band weakens, while that of 0.5-1 year frequency had strengthens. The directions of arrows at the significance level of 5% areas show that the lead/lag relations between house price and credit cycles change over time, while they also suggest that house price cycles lead credit for most of time and frequency domains.

From Figure A3, the 3-6 year frequency band has high and significant coherence between house price and GDP, especially the time period after 2005. The plotted arrows suggest that house prices lead GDP in most of the sample periods and frequencies.

Finally, Figure A4 shows that the 4-8 year frequency band has high and significant coherence between credit and GDP. Also, after the year 2005, coherence of the 1-3 year frequency band strengthens. As for the phase differences at the significance level of 5% areas, the directions of arrows shows that the lead/lag relations between credit cycles and GDP change over time.

Given the Wavelet analysis, the results of wavelet coherence are less decisive, while the phase difference gives us a better picture that house prices lead both credit and GDP in most of the time and frequency domains. In order to compare the results with the Multivariate STSM, we compute the means of wavelet coherences and phase differences for each time and frequency. We find that house price and credit has the highest means of wavelet coherence, and that house price cycles lead both credit and GDP cycles, and GDP leads credit cycles. These results are consistent with our Multivariate STSM.

C. Random Forest and Boosting

We now provide specifications of these two approaches and the criteria for variable importance and model evaluation.

C.1 Random Forest

Via decision trees, we can split the data into various nodes R_m and their corresponding probabilities p_m , where $m = 1, \dots, M$. Thus, the probability of downturn of those observations at the node \widehat{R}_m is given by

$$\widehat{p}_m = \frac{\sum_{t \in \widehat{R}_m} q_{t+h}}{\sum_{t \in \widehat{R}_m} 1}, \quad (1)$$

and the probability of forecasted downturn by the decision tree is given by

$$\widehat{TR}(x_t) = \sum_{m=1}^M \widehat{p}_m I(x_t \in \widehat{R}_m), \quad (2)$$

where q_t is a binary variable indicating an upturn or downturn (0 or 1), x_t is a $J \times 1$ vector of macroeconomic variables; the macroeconomic variables are seasonally and HP filtered, and then standardized so that their means are zero and standard errors are 1. Finally, we use the first difference of macroeconomic variables as predictors. $I(x_t \in \widehat{R}_m)$ is the indicator function for those observations classified as \widehat{R}_m . We use Gini Impurity (GI) to measure the probability of misclassifying an observation:

$$GI = 2p_a(1 - p_a), \quad (3)$$

where p_a is the ratio of observations at node R_a exhibiting downturns. Thus, $GI = 0$ if all observations at node R_a exhibit either downturns or upturns; and $GI = 0.5$ (the maximum value) if half of the observations at node R_a are in downturns and the other half are in upturns.

Next, Gini Gain (GG) measures the gains from classification after each data split, calculated by subtracting the weighted impurities of the nodes from the original impurity,

$$GG(R_a, R_b) = GI(R_a \cup R_b) - 0.5[GI(R_a) + GI(R_b)], \quad (4)$$

where $GI(R_a \cup R_b)$ is the Gini Impurity before classification, while $GI(R_a)$ and $GI(R_b)$ are respectively the Gini Impurity after splitting into nodes R_a and R_b . $GG(R_a, R_b)$ will be larger if the split improves the classification of downturns and upturns. Thus, when training a decision tree, the best split is chosen by maximizing the Gini Gain. We select the variable x_j and its corresponding threshold τ to maximize the Gini Gain:

$$\widehat{\tau}_j^s = \max_{\tau_j^s} GG(R_a, R_b),$$

where s represents the number of split, $s = 1, \dots, S$.

After repeated split of observations, the decision tree will be split into M nodes, $\{\widehat{R}_m\}_{m=1}^M$, with their corresponding probabilities being in downturns, $\{\widehat{p}_m\}_{m=1}^M$. Then, we can calculate the probability of forecasted downturn by the decision tree $\widehat{TR}(x_t)$ in (2).

Suppose there are D ensemble of decision trees, then the probability of forecasted downturn by the decision tree d , $d = 1, \dots, D$, is denoted by

$$\widehat{TR}_d(x_t) = \sum_{m=1}^M \widehat{p}_m^d I(x_t \in \widehat{R}_m^d),$$

then the probability of forecasted downturn by random forest is the averaged predictions of the ensemble of decision trees:

$$\widehat{RF}(x_t) = \frac{1}{D} \sum_{d=1}^D \widehat{TR}_d(x_t).$$

To evaluate the importance of a macroeconomic variable in fitting the downturns of financial cycles under random forest, we follow Breiman (2001) in using the measure Mean Decrease Gini (MDG) or GINI Importance (GI), based on the Gini Impurity used for the calculation of splits during training:

$$MDG(j) = \frac{1}{D} \sum_{d=1}^D \sum_{s=1}^{S_d} GG(\widehat{\tau}_j^s),$$

where $\sum_{s=1}^{S_d} GG(\widehat{\tau}_j^s)$ is the gains from S splits for variable j , $j = 1, \dots, J$. for the decision tree d . A variable is more important relative to others if the metric is larger.

C.2 Boosting

Boosting is a learning algorithm based on the idea of creating an accurate learner by combining many so-called “weak learners.” We follow Friedman and Hastie (2000) and Friedman (2001) by using a popular approach – Gradient boosting, which interprets boosting as a method for function estimation from the perspective of numerical optimization in a function space. We begin by defining the loss function $L(q, F(x))$, where q is a binary

variable indicating an upturn or downturn, x_t is a vector of macroeconomic variables, and $F(x)$ is called a “strong learner.” We define the function estimates at boosting iteration $n = 1, \dots, N$, to be $F_n(x)$.

Initializing the function estimate $F_0(x)$ at $n = 0$, with the initial value set to be a constant.

Raising the number of iterations n by 1, we compute the negative gradient of the loss function evaluated at the function estimate of the previous iteration:

$$\mathbf{u}_n = \{u_{n,t}\}_{t=1,\dots,T} = -\frac{\partial L(q_t, F(x_t))}{\partial F(x_t)} \Big|_{F=\widehat{F}_{n-1}(x_t)}, t = 1, \dots, T.$$

Let $f_n(x, \theta_n)$ be the weak learner of n^{th} iteration, θ_n is the set of parameters. We then estimate the weak learner $\widehat{f}_n^\kappa(x)$ by choosing a gradient descent step size κ that minimizes the residual sum of squares between $u_{n,t}$ and $\widehat{f}_n^\kappa(x_t, \theta_n)$:

$$\kappa = \arg \min_{\kappa} \sum_{t=1}^T \left(u_{n,t} - \widehat{f}_n^\kappa(x_t, \theta_n) \right)^2.$$

Thus, we can update the strong learner by adding the best-fitting weak learner to the function estimate of the previous iteration $n - 1$:

$$\widehat{F}_n = \widehat{F}_{n-1} + \delta_n \widehat{f}_n^\kappa,$$

where δ_n is the weight for the weak learner of iteration n . Finally, repeat the above procedure for the pre-specified number of iteration N .

To evaluate the importance of a macroeconomic variable in fitting the downturns of financial cycles under boosting, we use the measure Relative Influence (RI), which randomly permutes each predictor variable at a time and computes the associated reduction in predictive performance:

$$RI(j) = \frac{1}{N} \sum_{n=1}^N \widehat{i}_n^2 \cdot \mathbf{1}(\nu(x^n) = j),$$

where $\nu(x^n)$ is the splitting variable associated with node n , and $\mathbf{1}(\nu(x^n) = j)$ is the indicator function of iteration n for variable j , $j = 1, \dots, J$. \widehat{i}_n^2 is the corresponding empirical improvement in squared error as a result of the split, which serves as a weight for indicator function of iteration n . A variable is more important relative to others if the metric is higher.

References

- [1] Friedman, J. H. (2001), “Greedy function approximation: A gradient boosting machine,” *Annals of Statistics*, 29(5), 1189-1232.
- [2] Friedman, J.H. and T. Hastie (2000), “Additive logistic regression: a statistical view of boosting,” *Annals of Statistics*, 28(2), 337–407.
- [3] Grinsted, A., J.C. Moore, and S. Jevrejeva (2004), “Application of the cross wavelet transform and wavelet coherence to geophysical time series,” *Nonlinear Processes in Geophysics*, 11(5/6), 561–566.
- [4] Torrence, C. and G.P. Compo (1998), “A practical guide to wavelet analysis,” *Bulletin of the American Meteorological Society*, 79(1), 61–78.

Figure A1 The Wavelet Phase Differences

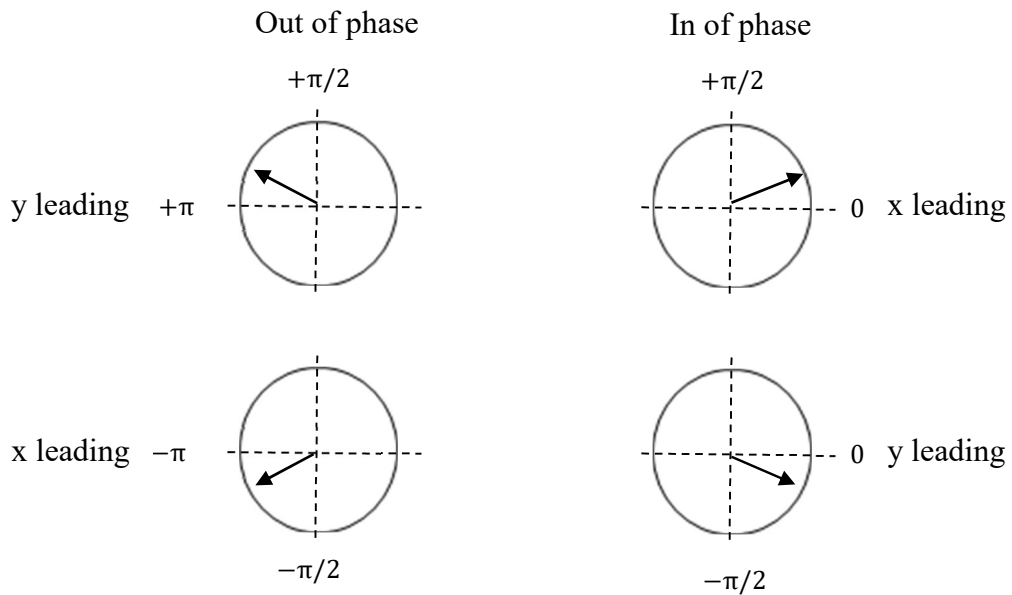
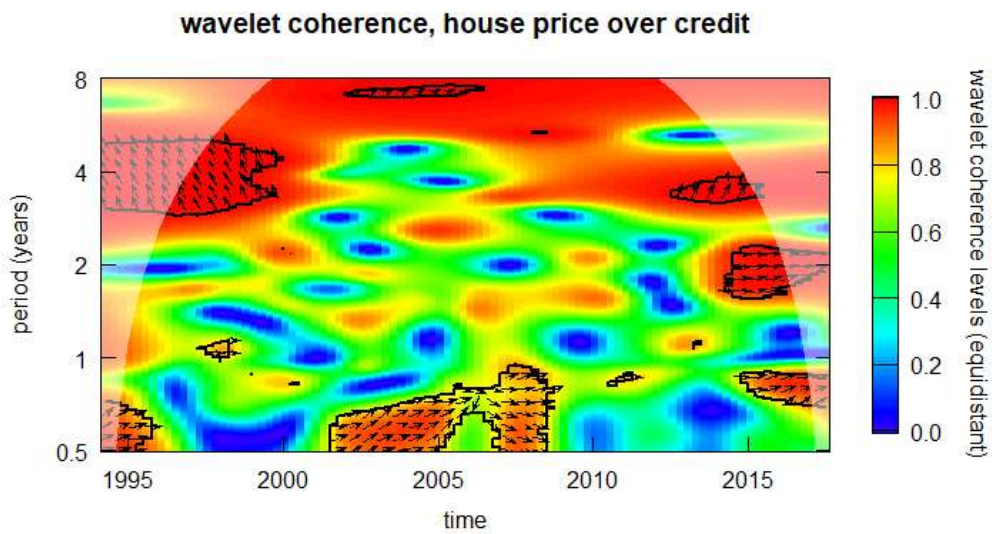
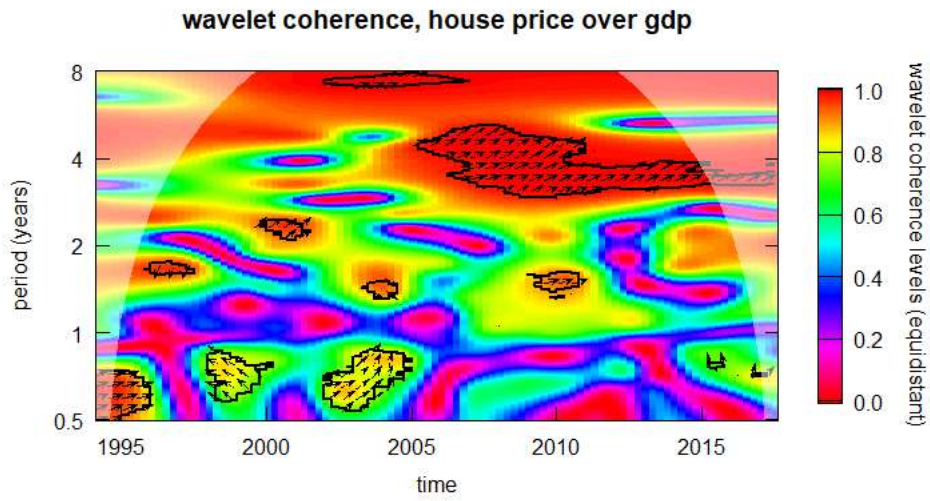


Figure A2 The Wavelet Coherence: House Price over Credit



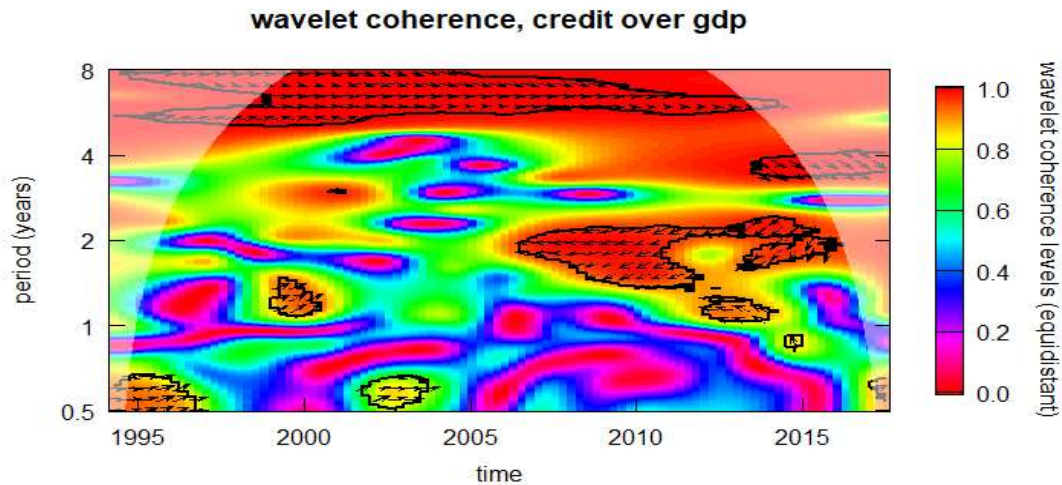
Note: The solid black line contours the significance level of 5% for the coherence: of house price over credit. The white area is the cone of influence. Plotted arrows show the phase differences of x over y at significant periods.

Figure A3 The Wavelet Coherence: House Price over GDP



Note: The solid black line contours the significance level of 5% for the coherence: of house price over credit. The white area is the cone of influence. Plotted arrows show the phase differences of x over y at significant periods.

Figure A4 The Wavelet Coherence: Credit over GDP



Note: The solid black line contours the significance level of 5% for the coherence: of house price over credit. The white area is the cone of influence. Plotted arrows show the phase differences of x over y at significant periods.